THE MEASURED VARIATION OF THE DEBYE-WALLER FACTOR OF ALUMINUM FROM 295K TO 815K BY USING THE ENERGY DISPERSIVE X-RAY DIFFRACTION TECHNIQUE

by

SON-HA NGUYEN, B.Sc.

A Thesis
submitted to the Department of Physics
in partial fulfillment of the requirement
for the degree of
Master of Science

August 1992
Brock University
St. Catharines, Ontario

ACKNOWLEDGEMENTS

I would like to thank my supervisor, Dr. J. A. Moore, for his teaching and his kindness. My thanks are also due to Dr. F. P. Koffyberg, Dr. B. Mitrovic and Dr. F. S. Razavi for their help and their support.

ABSTRACT

The Energy Dispersive X-ray Diffraction System at Brock University has been used to measure the intensities of the diffraction lines of aluminum powder sample as a function of temperature. At first, intensity measurements at high temperature were not reproducible. After some modifications have been made, we were able to measure the intensities of the diffraction lines to 815K, with good accuracy and reproducibility. Therefore the changes of the Debye-Waller factor from room temperature up to 815K for aluminum were determined with precision. Our results are in good agreement with those previously published.

TABLE OF CONTENTS

LIST OF TABLES

LIST OF FIGURES

CHAPTER 1

INTRODUCTION

Atoms are regularly arranged in crystals with an interatomic distance of a few angstroms, thus they may scatter and diffract x-ray radiation. Diffracted beams occur when the Bragg law is satisfied:

$$2d\sin\theta = n\lambda,$$

where θ is the glancing angle for the incident and diffracted x-ray radiation, d is the interplanar spacing of the reflecting planes, n is an integer, and λ is the wavelength of the x-ray radiation. The x-ray photon energy is:

$$E = \frac{hc}{\lambda},$$

where h is a Planck's constant and c is the speed of light.

For powder samples, the diffraction can be observed in two ways: use monochromatic x-ray radiation and measure the intensity of scattered radiation as a function of scattering angle 2θ; use polychromatic x-ray radiation and measure the intensity of scattered radiation as a function of energy E, keeping 2θ fixed.The former is called Angle Dispersive X-ray Diffraction (ADXD) and the latter is called Energy Dispersive X-ray

Diffraction (EDXD).

Both methods can make precise intensity measurements of diffraction lines. The ADXD method has an excellent d space resolution, so it is the preferred method to determine the structure of complex crystalline materials with closely spaced diffraction lines.The concept of EDXD has been known for a long time. However, it only became practical after the development of the semiconductor photon spectrometer with sufficient energy resolution. Giessen & Gordon [1] were the first to report measurements of the intensity of x-ray diffraction by the EDXD method. They used a white x-ray source from an Fe anode combined with a lithium drifted silicon detector, Si(Li), to measure the scattered x-ray photon energies and intensities. The measurements were performed on sheet samples of polycrystalline Cu, Ag ,Re, Pt, and Au. Because of the limited d space resolution of EDXD when combined with a Si(Li) photon spectrometer, there has been rather little application of EDXD to the determination of the structure of crystalline materials. The EDXD method has the simplest experimental arrangement since the scattering angle 2θ is constant. It is therefore particularly useful in high temperature or high pressure measurements on simple structures, in which the sample chamber may restrict the range of angular scan. It also has been used effectively to study the Structural Relaxation and the Radial Distribution Function of amorphous materials [2,3], since for these non-crystalline materials, closely spaced, sharp diffraction lines are not present and the limited d space resolution provided by EDXD with a Si(Li) photon spectrometer is quite adequate. Also the EDXD method can measure diffraction intensities for scattering vectors $\mathbf{q}$ with high magnitude

because its high energy radiation, and this is very useful for diffraction studies on amorphous materials. The magnitude of **q** is given by:

$$q = \frac{4\pi}{hc} E \sin\theta ,$$

$$q = 10.14\ E \sin\theta \quad ,$$

where E is in KeV and q is in nm^{-1}.

Elyaseery [4] has installed an EDXD system at Brock University. To demonstrate its performance, he successfully measured intensities of diffraction lines for aluminum powder at room temperature. However, his measurements at higher temperatures were not consistently reproducible.

The principal objective in this thesis project was to measure the intensities of the diffraction lines of aluminum powder as a function of temperature and so determine the Debye-Waller factor of aluminum with precision, by using the EDXD system at Brock University. The reason for our choice of aluminum was that it has a low melting point so that only a simple heating arrangement was required. Also the Debye-Waller factor of aluminum has been studied theoretically [5,6] and has been measured by several different techniques: the ADXD technique [7, 8, 9, 10,], the neutron diffraction technique [11], the Mössbauer effect technique [12], but not by the EDXD method. The measurement of the Debye-Waller factor of aluminum would therefore further demonstrate the usefulness of the EDXD system at Brock University.

The theory of x-ray diffraction shows that the intensity of a diffracted beam is a function of temperature. The thermal energy

increases the vibration of atoms about their equilibrium positions in a crystal lattice, this motion reduces the intensity of diffraction and increases the intensity of the Thermal Diffuse Scattering (TDS). If I_R, I_T are the intensities of a diffraction line at room temperature and at temperature T respectively and M_R, M_T are corresponding Debye-Waller factors, then we can write:

$$\frac{I_R}{I_T} = \exp 2(M_T - M_R),$$

where

$$M_T = B_T \frac{\sin^2\theta}{\lambda^2}$$

and B_T is a function of the mean square vibration of the crystal atoms.

Theoretically, Killean & Lisher [5] have shown that the variation of the Debye-Waller factor of aluminum can be described by means of the nearest neighbor central force pair interaction given by Killean [14]. Shukla & Hubschle [6] have presented theoretical results for the quasi-harmonic and anharmonic contributions to the Debye-Waller factor of aluminum in the temperature range from 300K to 850K.

Experimentally, the Debye-Waller factor of aluminum was first measured in 1947 by Owen & Williams [7], the measurements of the intensities of the x-ray diffracted beams were not corrected for TDS . Chipman [8] scattered x-rays from aluminum powder samples. Nicklow & Young [9] measured x-ray intensities scattered from aluminum single crystals in the low temperature range (100K - 300K). Dingle & Medlin [10] obtained x-ray intensities of fifty-eight reflections from each of two aluminum single crystals in the temperature range from 293K to 559K.

The Debye-Waller factor has also been determined by techniques other than x-ray diffraction. MacDonald [11] used the neutron diffraction method to measure the intensities of a neutron beam scattered from an aluminum single crystal. He was able to collect a complete set of intensity data out to the (620) reflection in the temperature range from 300K to 860K, he used the Wilson plot [13] to determine the Debye-Waller factor $B_{(T)}$. Martin & O'Connor [12] used the Mössbauer effect on a large aluminum single crystal to measure the Debye-Waller factor up to 900K. The advantage of the Mössbauer technique is that it can separate the TDS from diffraction, so TDS can be eliminated from the intensities of Bragg peaks.

This thesis contains in Chapter 2 the theory: the Bragg law, calculation of the intensity of x-rays diffracted from powder crystals, the influence of temperature, and the TDS; in Chapter 3 a description of the EDXD system: intensity of a diffraction line as a function of (E, θ, T), the instrumental set up; in Chapter 4 the experimental development and results: determination of the intensity of a diffraction peak, the stability of the incident beam and the reproducibility of absolute intensities at room temperature, the intensities of diffraction lines as a function of temperature from unpressed samples, some modifications, determination of the variation of the Debye-Waller factor of aluminum with temperature; and in Chapter 5 the conclusion.

CHAPTER 2

THEORY

The scattering of x-rays from an atom is due to the electromagnetic interaction between the radiation and atomic electrons. Classically, the oscillating electric field of an x-ray beam will set any electron which it encounters into oscillatory motion about its mean position. An oscillating electron which is continuously accelerating and decelerating during its motion emits an eletromagnetic wave. In this sense, an electron is said to scatter x-rays, the scattered beam is simply the beam radiated by an electron under the action of the incident beam. We are only interested in the coherent scattering, in which the scattered beam has the same wavelength as the incident radiation, since only this is effective in forming interference maxima.

2.1 Diffraction conditions.

If **a**, **b**, and **c** are primitive vectors of the crystal lattice, then we can define primitive vectors of the reciprocal lattice **a***, **b*** and **c*** as:

$$\mathbf{a}^* = 2\pi \frac{\mathbf{b}\times\mathbf{c}}{\mathbf{a}.\mathbf{b}\times\mathbf{c}} , \qquad \mathbf{b}^* = 2\pi \frac{\mathbf{c}\times\mathbf{a}}{\mathbf{a}.\mathbf{b}\times\mathbf{c}} , \qquad \mathbf{c}^* = 2\pi \frac{\mathbf{a}\times\mathbf{b}}{\mathbf{a}.\mathbf{b}\times\mathbf{c}} .$$

For each set of (hkl) planes in the crystal lattice, there is a reciprocal lattice vector:

$$\mathbf{G} = h\mathbf{a}^* + k\mathbf{b}^* + l\mathbf{c}^*,$$

which is perpendicular to the planes, where h, k, l are the Miller indices of the planes.

The set of reciprocal lattice vectors **G** determines the possible x-ray diffractions, and also enters the Fourier series expression for the periodic electron density of the crystal lattice. The diffracted beam directions may be determined as follows. Following C. Kittel [15], Fig. 2.1 shows that the difference in phase factors between beams scattered from volume elements dv, position vector **r** apart is:

$$\exp[i(\mathbf{k} - \mathbf{k}').\mathbf{r}] ,$$

where **k** and **k'** are the wave vectors of the incident beam and the diffracted beam respectively.

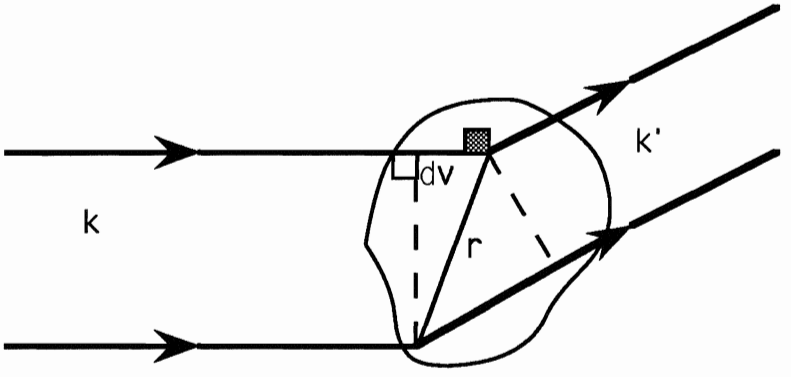

Fig. 2.1 The scattering from volume elements, distance **r** apart.

The amplitude of the wave scattered from a volume element is proportional to the local electron density n(**r**), so the total amplitude A of the scattered waves in the direction **k'** is proportional to the integral over the crystal of n(**r**)dv times the phase factor exp[i(**k** - **k'**).**r**]:

$$A = \int n(\mathbf{r}) dv \exp(-i\mathbf{q}.\mathbf{r}) , \qquad (2.1)$$

where $\mathbf{q} = \mathbf{k}' - \mathbf{k}$ is the scattering vector, $n(\mathbf{r})$ is periodic in the crystal lattice and by using the reciprocal lattice vector **G**, it can be expressed by a Fourier series:

$$n(\mathbf{r}) = \sum_{\mathbf{G}} n_{\mathbf{G}} \exp(i\mathbf{G}.\mathbf{r}) .$$

Thus: $$A = \sum_{\mathbf{G}} \int dv \, n_{\mathbf{G}} \exp[i(\mathbf{G} - \mathbf{q}).\mathbf{r}] ,$$

$A = Vn_{\mathbf{G}}$ when $\exp[i(\mathbf{G} - \mathbf{q}).\mathbf{r}] = 1$ and A is very small otherwise.

So $$\mathbf{q} = \mathbf{G} \qquad (2.2)$$

is the condition for diffraction.

In elastic scattering, the photon energy, $h\omega/2\pi$, is conserved. Thus the magnitude of **k** and **k'** are equal: $|k| = |k'| = 2\pi/\lambda$.

If we take a dot product of both sides of Eq. (2.2) with **a** , **b** , **c** of the crystal lattice respectively, we obtain the three Laue conditions for diffraction:

$$\mathbf{a}.\mathbf{q} = 2\pi h , \qquad \mathbf{b}.\mathbf{q} = 2\pi k , \qquad \mathbf{c}.\mathbf{q} = 2\pi l . \qquad (2.3)$$

Because $|k| = |k'|$, and from Eq. (2.2), we may also rewrite the condition for diffraction as follows:

$$(\mathbf{k} + \mathbf{G})^2 = k^2 ,$$

or $$2\mathbf{k}.\mathbf{G} + G^2 = 0.$$

Notice that **-G** is also a reciprocal lattice vector, thus we can write:

$$2\mathbf{k}.\mathbf{G} = G^2 . \qquad (2.2a)$$

The spacing between parallel lattice planes normal to the direction of $\mathbf{G} = h\mathbf{a}^* + k\mathbf{b}^* + l\mathbf{c}^*$ is:

$$d_{(hkl)} = \frac{2\pi}{|\mathbf{G}|} ,$$

thus Eq. (2.2a) may be rewritten as:

$$2(2\pi/\lambda)\sin\theta = 2\pi/d(hkl),$$

or $$2d\sin\theta = \lambda, \qquad (2.4)$$

where θ is the angle between **k** and the reflecting plane (hkl).

This is Bragg's Law for diffraction.

Eqs. (2.2), (2.3) and (2.4) are various statements of the condition for x-ray diffraction.

2.2 Calculation of the intensity of x-ray diffracted from powder crystals.

We start with Eq. (2.52) from R. C. James [16]:

$$P = I_o Q dv , \qquad (2.5)$$

where P is the power of a diffracted beam, integrated through the diffraction peak, at the angle 2θ from the incident direction, from a small crystal element of volume dv, in which absorption may be neglected. I_o is the energy incident per unit area per unit time. Eq. (2.5) shows as is expected, that P is proportional I_o and dv.To find the expression for Q, we need the derivation of Eq. (2.5). The following is a summary of detailed derivation given by R. C. James [16]:

Consider the wave reflected from a plane containing n unit cells per unit area, in the direction of 2θ with respect to the incident beam. All unit cells in the plane scatter x-rays. By superimposing the waves scattered from all the unit cells, the amplitude of the reflected wave, g, including phase factor, relative to that of the incident wave is given by (a complex number):

$$g = i \frac{n\lambda}{\sin\theta} F \left(\frac{e^2}{mc^2}\right) \quad , \tag{2.6}$$

where λ is the incident beam wavelength, e^2/mc^2 is the amplitude at unit distance of the beam scattered by an electron from incident radiation which is polarized with the electric vector perpendicular to the incident plane, and i is the imaginary number.

The structure factor F is the amplitude of the wave scattered by a unit cell relative to the wave scattered by an electron, F is given by:

$$F = \sum_j f_j \exp(i\mathbf{q}.\mathbf{r}_j) \, ,$$

where f_j is the atomic scattering factor of the atom j located at $\mathbf{r}_j$ in the unit cell. The summation is over all atoms in the unit cell. The atomic scattering factor f is the amplitude of the wave scattered from an atom relative to that scattered by an electron. f is given by:

$$f = \int dv\, n(\mathbf{r}) \exp(i\mathbf{q}.\mathbf{r}) ,$$

where $n(\mathbf{r})$ is the electron density for the atom.

We now consider the amplitude of the beam reflected by a number of planes. Each plane scatters an amplitude g given by Eq. (2.6), but there is a phase difference between the amplitudes contributed by successive planes, separated by a distance a, equal to $4\pi a \sin\theta/\lambda$. Let θ_B be the angle corresponding to exact agreement in phase between the reflections from successive planes, if the angle differs from θ_B by a small angle ε, the phase difference becomes:

$$\delta = \frac{4\pi a \varepsilon}{\lambda} \cos\theta_B .$$

If the amplitude of the incident radiation is A_o, and that of the resultant reflected wave from p planes is A, then:

$$\frac{A}{A_o} = g\,(1 + e^{-i\delta} + \ldots\ldots + e^{-ip\delta}) = g\,\frac{1 - e^{-ip\delta}}{1 - e^{-i\delta}} \quad .$$

Let I_o and I_ε be the corresponding intensities:

$$R(\varepsilon) = \frac{I_\varepsilon}{I_o} = |g|^2 \frac{\sin^2 pB\varepsilon}{\sin^2 B\varepsilon} ,$$

where $$B = \frac{2\pi a}{\lambda}\cos\theta_B.$$

To calculate the reflected power of a diffraction peak, we integrate $R(\varepsilon)$ over the range of appreciable reflection in the region of the intensity maximum. This gives:

$$P = I_o Q_1 dv,$$

where dv is the volume of the small crystal ,

$$Q_1 = \frac{N^2\lambda^3}{\sin 2\theta}|F|^2\left(\frac{e^2}{mc^2}\right)^2$$

and N is the number of unit cells per unit volume, for the polarized incident beam with the electric vector perpendicular to the incident plane.

If the electric vector is parallel to the incident plane, then:

$$P = I_o Q_2 dv,$$

where $$Q_2 = Q_1 \cos^2 2\theta .$$

If the incident beam is unpolarized, then:

$$P = I_o Q dv,$$

which is Eq. (2.5).

where $$Q = \frac{1}{2}(Q_1 + Q_2) = \frac{N^2\lambda^3}{\sin 2\theta}|F|^2\left(\frac{e^2}{mc^2}\right)^2\frac{1}{2}(1 + \cos^2 2\theta). \qquad (2.7)$$

For a crystalline powder sample, containing M particles,the number of particles having the correct orientation for diffraction at the

glancing angle θ is $\frac{1}{2} M\cos\theta d\theta$. If $<P(\theta)>$ is the average reflecting power of a particle, then the total energy reflected into a halo (Fig. 2.3) may be obtained by:

$$P = \frac{1}{2} I_o M \cos\theta_o \int <P(\theta)> d\theta = \frac{1}{2} I_o M Q \cos\theta_o <dv> .$$

Put $M<dv> = V$, the volume of the powder sample to be seen by the incident beam. We have also to take into account the possible number of sets of planes with different Miller indices but having the same spacing, and so reflecting into the same halo. Let the number of equivalent planes be the multiplicity factor p, then:

$$P = \frac{1}{2} I_o p Q \cos\theta_o V. \qquad (2.8)$$

Only a portion of the reflected halo enters the detector with a slit of the height t. To calculate the reflected power of that portion, we multiply Eq. (2.10) with $t/2\pi r\sin 2\theta$, (Fig. 2.2):

$$P = I_o \frac{ptQ}{8\pi r \sin\theta} V. \qquad (2.9)$$

Equation (2.9) refers to a powdered sample of total volume V which is sufficiently small that no significant absorption occurs. We now consider the powdered crystal tablet sufficiently thick that the incident beam is partially absorbed. Let μ be the linear absorption coefficient of the sample, and S is the cross section of the incident beam. The result of the integration shows the effective volume of the sample seen by the beam is:

$$V = \frac{S}{2\mu}.$$

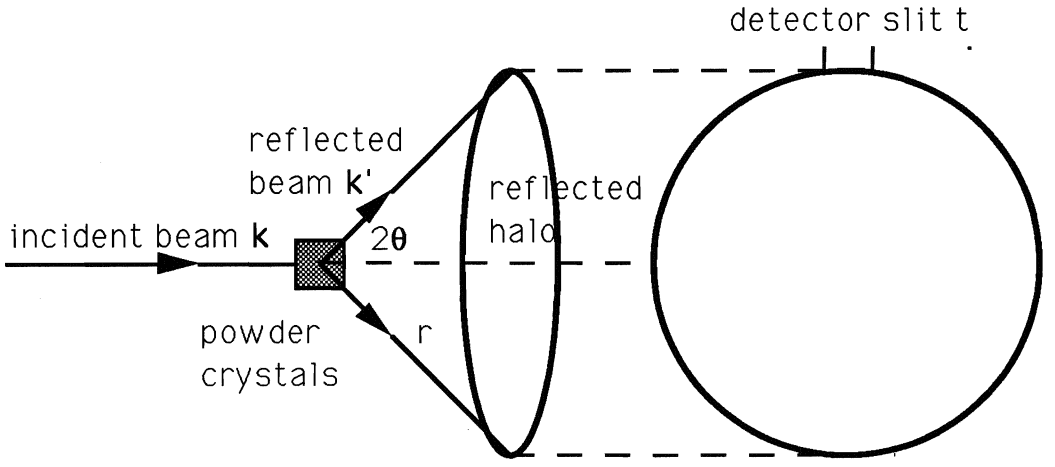

Fig. 2.2 X-ray diffraction from a crystal powder sample. The detector has a slit t high located at a distance r from the crystal element.

We finally have the formula to calculate the reflected power of a diffracted beam for a thick tablet, received by the detector of slit t:

$$P = I_o S \frac{ptQ}{16\pi r \mu \sin\theta},$$

or

$$P = I_o \frac{N^2 S \lambda^3}{32\pi r} pt |F|^2 \left(\frac{e^2}{mc^2}\right)^2 \frac{1+\cos^2 2\theta}{\sin^2\theta\cos\theta} \frac{1}{2\mu} \qquad (2.10)$$

for a static periodic lattice.

2.3 The influence of temperature.

So far we only have considered a crystal that is a stationary assemblage of atoms bound together in a periodic pattern. We now consider how the situation is modified under the influence of thermal

energy in which all atoms are vibrating about their equilibrium positions with amplitudes increasing as temperature goes up. These vibrations will affect the relative coordinates of atoms and hence the intensity of a diffracted beam. Only the vibration which is perpendicular to the reflecting planes will affect the diffraction intensity. To describe the effect of temperature and atomic vibration, consider the structural factor of a unit cell in a one dimensional lattice, lattice constant a, where the atom j^{th} has a mean fractional coordinate x_j and at some instant of time, an absolute dispacement u_j from that position [17], we can write the structural factor corresponding to index h as:

$$F_h = \sum_1^N f_j \exp\{2\pi i h(\frac{u_j}{a} + x_j)\} ,$$

$$= \sum_1^N f_j \exp 2\pi i h \frac{u_j}{a} \exp 2\pi i h\, x_j \ .$$

The actual structure amplitude in a direction corresponding to h will be a time and space average since u_j varies from one unit cell to the next and, within one unit cell, varies with time. Thus at some temperature T, the structural factor is:

$$(F_h)_T = \sum_1^N f_j < \exp 2\pi i h \frac{u_j}{a} > \exp 2\pi i h\, x_j \quad , \qquad (2.11)$$

where $< \exp 2\pi i h \frac{u_j}{a} >$ is the average value of displacement term. It is practical to assume that u_j is small:

$$u_j/a << 1,$$

$$< \exp 2\pi i h \frac{u_j}{a} > \approx 1 + 2\pi i h \frac{<u_j>}{a} - 2\pi^2 h^2 \frac{<u_j^2>}{a^2} \cdot$$

For simple harmonic vibration, $< u_j > = 0$:

$$< \exp 2\pi i h \frac{u_j}{a} > \approx 1 - 2\pi^2 h^2 \frac{<u_j^2>}{a^2} ,$$

$$\text{or} \quad < \exp 2\pi i h \frac{u_j}{a} > \approx \exp(- 2\pi^2 h^2 \frac{<u_j^2>}{a^2}) \cdot \qquad (2.12)$$

Substitute Eq. (2.12) into Eq. (2.11) with $\frac{h}{a} = \frac{2\sin\theta}{\lambda}$, we have:

$$(F_h)_T = \sum_1^N f_j \exp(-8\pi^2 <u_j^2> \frac{\sin^2\theta}{\lambda^2}) \exp 2\pi i h x_j.$$

It can be seen that the result of the thermal motion of atoms is effectively to modify their scattering factors:

$$(f_j)_T = f_j \exp(-8\pi^2 <u_j^2> \frac{\sin^2\theta}{\lambda^2}) \cdot$$

In the three dimensional case, the result has the same form except that we replace $<u_j^2>$ by $<u_{\perp j}^2>$ which is the mean square displacement of an atom in the direction perpendicular to the reflecting planes.

If $B_j = 8\pi^2 <u_{\perp j}^2>$, then:

$$(f_j)_T = f_j \exp(-B_j \frac{\sin^2\theta}{\lambda^2}) \cdot$$

The quantity B_j is known as the temperature factor of the j^{th} atom. It is usually sufficient to assume that thermal vibrations are isotropic and that values of B are the same for all atoms. In that case, we have:

$$(F_{hkl})_T = F_{hkl} \exp(-B \frac{\sin^2\theta}{\lambda^2}).$$

Let $M = B \frac{\sin^2\theta}{\lambda^2}$, then:

$$(F_{hkl})_T = F_{hkl} \exp(-M). \qquad (2.13)$$

The factor e^{-M} by which the observed intensities are reduced by thermal vibration, is known as the Debye-Waller factor. The dependence of B on the absolute temperature T has been theoretically investigated by Debye and corrected by Waller [18] for cubic structure crystalline elements. If Θ is the Debye characteristic temperature of a material and $x = \Theta / T$, then:

$$B_{(T)} = \frac{6h^2}{mk\Theta} \{ \frac{\phi(x)}{x} + \frac{1}{4} \},$$

where:

m: the atomic mass,

h: Planck's constant,

k: Boltzman's constant,

and $\phi(x) = \frac{1}{x} \int_0^x \frac{\xi}{\exp\xi - 1} d\xi$.

To summarize, for a polycrystalline sample, made up of randomly oriented grains, in the form of a flat plate of sufficient thickness to absorb the incident beam, making equal angles with the incident and diffracted beams, the expression for the diffracted beam from this sample [from Eq. (2.10)] is given by:

$$I = I_o \frac{N^2\lambda^3}{32\pi r} pt |F|^2 \left(\frac{e^2}{mc^2}\right)^2 \frac{1+\cos^2 2\theta}{\sin^2\theta\cos\theta} \frac{e^{-2M}}{2\mu}, \qquad (2.14)$$

where now I, I_o represent the intensities of the diffracted beam and the incident beam repectively.

2.4 The experimental determination of the Debye-Waller factor.

The Debye-Waller factor $B_{(T)}$ is experimentally determined as follows:

We can rewrite Eq. (2.14) for a (hkl) line as:

$$I_{hkl} = K\, H(hkl, \theta) \exp\left(-2B_{(T)} \frac{\sin^2\theta}{\lambda^2}\right),$$

where $$K = I_o \frac{N^2\lambda^3}{32\pi r} \left(\frac{e^2}{mc^2}\right)^2 \frac{t}{2\mu}$$

and $$H(hkl, \theta) = p |F|^2 \frac{1+\cos^2 2\theta}{\sin^2\theta\cos\theta}.$$

Rearrange the terms and take the natural logarithm of both sides:

$$\ln \frac{I_{hkl}}{H(hkl, \theta)} = \ln K - 2B_{(T)} \frac{\sin^2\theta}{\lambda^2}.$$

For a given temperature T, a plot of ln (I/H) as a function of $(\sin^2\theta/\lambda^2)$, called the Wilson plot [13], gives a straight line of slope -

$2B_{(T)}$ and an intercept of ln K.

Alternatively we can experimentally determine the change of the Debye-Waller factor from room temperature to a temperature T. We write the formula for the intensity of a diffraction line (hkl) at room temperature:

$$I_{hkl(R)} = K\, p\, |F|^2 \frac{1+\cos^2 2\theta}{\sin^2\theta\cos\theta} \exp(-2M_R), \qquad (2.15a)$$

and that at temperature T:

$$I_{hkl(T)} = K\, p\, |F|^2 \frac{1+\cos^2 2\theta}{\sin^2\theta\cos\theta} \exp(-2M_T). \qquad (2.15b)$$

Divide Eq. (2.15a) by Eq. (2.15b) and take the natural logarithm of both sides (drop the subscripts hkl):

$$\ln \frac{I_R}{I_T} = 2(M_T - M_R),$$

$$= 2(B_T - B_R) \frac{\sin^2\theta}{\lambda^2}.$$

Put $\Delta B_{(T)} = B_T - B_R$,

then $$\ln \frac{I_R}{I_T} = 2\Delta B_{(T)} \frac{\sin^2\theta}{\lambda^2}. \qquad (2.16)$$

For a given T, a plot of $\ln \frac{I_R}{I_T}$ versus $\frac{\sin^2\theta}{\lambda^2}$ yields a straight line through the origin of slope $2\Delta B_{(T)}$.

2.5 The Thermal Diffused Scattering (TDS).

The thermal motion of atoms in a crytal lattice causes a weakening of the intensities of the Bragg lines and an increase in the total amount of the TDS.TDS of x-rays scattered by a crystal has maxima at those angles of scattering at which the Bragg diffraction maxima occur in the elastic scattering. The TDS in this region involves the exchange of energy by the x-ray with phonons present in the crystal [19]. For a typical case, the energy exchange may be about 10^{-8} eV. Such small changes can not be detected by x-ray spectrometric methods. But the Mossbauer effect with the recoiless emission and absorption of low energy γ-rays can detect such changes because the Mössbauer effect has an energy resolution as small as a few 10^{-8} eV [19,20, 21]. Fig. 2.3 shows the TDS of (440) lines at room temperature from an aluminum crystal detected by the Mössbauer effect.

For x-ray diffraction, the TDS correction σ is defined as:

$$\sigma = \frac{A_{TDS}}{A_{Bragg}},$$

where A_{TDS} represents the integrated intensity of the TDS and A_{Bragg} represents that of the Bragg peak above the TDS.

The corrected intensity of elastic scattering of the Bragg peak is:

$$A_{Bragg} = \frac{A_{meas}}{1+\sigma},$$

where A_{meas} is the intensity measured by a detector.

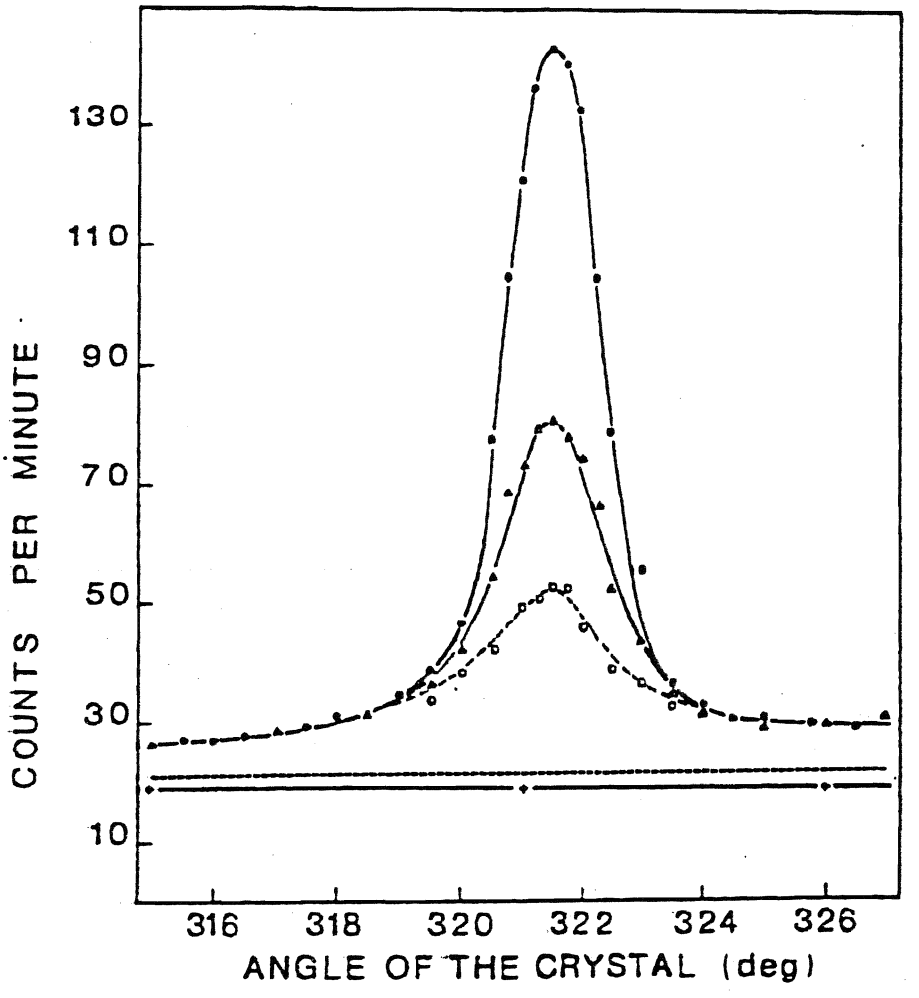

Fig. 2.3 The TDS of (440) reflection (open circles) from an aluminum crystal at room temperature, measured by Albanese and Ghezzi using the Mössbauer effect. Intensities when the absorber is in and out relative to the source are open triangles and closed circles respectively.

The formula to calculate the TDS correction σ has been derived by Willis [22] for single crystals. Paskin [23,24], Chipman & Paskin [25,26] have derived the empirical formula to calculate σ for a face centered

cubic powder crystals:

$$\sigma = (\pi/3)^{1/3} M_D a \Delta \, (\cos\theta)/\lambda \, , \qquad (2.17)$$

where :

M_D is the Debye-Waller factor,

a is the lattice constant,

θ is the Bragg angle,

λ is the X-ray wavelength,

Δ is the angular range of integration through the diffraction peak.

CHAPTER 3

THE ENERGY DISPERSIVE X-RAY DIFFRACTION SYSTEM

3.1 Energy Dispersive X-ray Diffraction (EDXD).

The Bragg condition for diffraction from a set of reflecting planes is given in Eq.(2.4):

$$2d\sin\theta = \lambda \ ,$$

λ can be written in terms of energy as:

$$\lambda = \frac{hc}{E} = \frac{12.4}{E} \ , \qquad (3.1)$$

where E is the photon energy in KeV and λ is in Å, then for EDXD, in which θ is constant and intensity is measured as function of energy, E, the Bragg law is rewritten in E by combining Eqs. (3.1) and (2.4) to give:

$$Ed = \frac{6.2}{\sin\theta} = \text{constant.} \qquad (3.2)$$

In Eq. (3.2), E is the energy of the diffraction peak corresponding to the planes of spacing d.

In this work, diffraction from powdered crystalline samples is used. The expression for the intensity of a diffracted beam from a powdered sample is given in Eq. (2.14):

$$I = I_o \frac{N^2\lambda^3}{32\pi r}\, pt \left(\frac{e^2}{mc^2}\right)^2 |F|^2 \frac{1+\cos^2 2\theta}{\sin^2\theta\cos\theta} \frac{e^{-2M}}{2\mu} . \qquad (3.3)$$

For the EDXD method, incident polychromatic radiation is used while the scattering angle 2θ of the system is fixed. Eq. (3.3) can be rewritten to be suitable for EDXD by expressing I_o and λ in terms of E. I_o can be replaced by $I(E)\Delta E$, the intensity of incident radiation in the energy interval ΔE. I(E) is the intensity of the incident polychromatic radiation per unit energy in the energy interval ΔE. ΔE corresponds to the effective angle of acceptance $\Delta\theta$ which equals the range of diffraction angles accepted by the detector. The relationship between ΔE and $\Delta\theta$ may be derived by taking the derivative of the energy E, with respect to the angle of diffraction θ of the EDXD Bragg relation, Eq. (3.2), this gives:

$$\frac{dE}{d\theta} = -\frac{hc}{2d\sin^2\theta}\cos\theta = -\frac{h.c}{2d\sin\theta}\frac{1}{\tan\theta},$$

$$= -\frac{E}{\tan\theta} .$$

So $$\Delta E = -\frac{E}{\tan\theta}\Delta\theta .$$

Also $$\lambda = \frac{hc}{E} .$$

From Eq. (3.3) , the intensity of a diffraction line can be rewritten in terms of energy of incident x-ray radiation:

$$I = I(E)\Delta E\left(\frac{hc}{E}\right)^3 \frac{N^2}{32\pi r}\left(\frac{e^2}{mc^2}\right)^2 pt\,|F|^2 \frac{1+\cos^2 2\theta}{\sin^2\theta\cos\theta} \frac{e^{-2M}}{2\mu(E)},$$

$$= I(E)\frac{\Delta\theta}{\tan\theta}\frac{(hc)^3}{E^2}\frac{N^2}{32\pi r}\left(\frac{e^2}{mc^2}\right)^2 pt\,|F|^2 \frac{1+\cos^2 2\theta}{\sin^2\theta\cos\theta} \frac{e^{-2M}}{2\mu(E)} .$$

$$= I(E)\frac{\Delta\theta}{E^2}\frac{N^2(hc)^3t}{32\pi r}\left(\frac{e^2}{mc^2}\right)^2 p\,|F|^2\,\frac{1+\cos^2 2\theta}{\sin^3\theta}\,\frac{e^{-2M}}{2\mu(E)} \quad . \qquad (3.4)$$

Put $$K = \frac{N^2(hc)^3t}{32\pi r}\left(\frac{e^2}{mc^2}\right)^2\Delta\theta\,,$$

we can write Eq. (3.4) as:

$$I = K\, I(E) p\,\frac{1}{E^2}|F|^2\,\frac{1+\cos^2 2\theta}{\sin^3\theta}\,\frac{e^{-2M}}{2\mu(E)} \qquad (3.5)$$

for calculating the intensity of a diffracted beam, energy E, measured by the EDXD method.

We measure intensity of a diffracted beam, I, as a function of temperature, T. For EDXD, Ed is constant [Eq.(3.2)] and the energy E of a diffraction peak is very slightly temperature dependent. So in Eq.(3.5), I(E), E^2, $|F|^2$ and $\mu(E)$ are all slightly temperature dependent. The dominant and only significant temperature dependent factor is e^{-2M}, where:

$$M = B\,\frac{\sin^2\theta}{\lambda^2} = B\,\frac{1}{4d^2}\,.$$

M is the Debye-Waller factor and B is a function of the mean square displacement of the crystal atoms from their equilibrium positions.

From Eq. (3.5), the intensity of a given diffraction line (hkl) at room temperature (R) is:

$$I_{(hkl)R} = K\,\frac{I(E)_R}{E_R^2}\; p\,|F|^2\, A\,\frac{e^{-2M_R}}{2\mu(E)_R}$$

and the intensity of (hkl) line at temperature (T) is:

$$I_{(hkl)T} = K \frac{I(E)_T}{E_T^2} p |F|^2 A \frac{e^{-2M_T}}{2\mu(E)_T},$$

where $$A = \frac{1+\cos^2\theta}{\sin^3\theta}.$$

Take the ratio of $I_{(hkl)R}$ and $I_{(hkl)T}$, and drop the subscript (hkl) :

$$\frac{I_R}{I_T} = \exp 2(M_T - M_R).$$

Take the natural logarithm of both sides and replace M by $B\frac{1}{4d^2}$, then:

$$\ln \frac{I_R}{I_T} = 2(B_T \frac{1}{4d_T^2} - B_R \frac{1}{4d_R^2}),$$

where d_R and d_T are spacings at room temperature and temperature T respectively.

For a cubic crystal:

$$d_{hkl}^2 = \frac{a^2}{h^2+k^2+l^2}$$ where a is lattice constant.

Therefore:

$$\ln \frac{I_R}{I_T} = 2(B_T \frac{a_R^2}{a_T^2} - B_R) \frac{1}{4d_R^2} \cdot \qquad (3.6)$$

Thus ln (I_R/I_T) is linearly dependant on $(1/4d_R^2)$, its slope is:

$$2B_T \frac{a_R^2}{a_T^2} - B_R ,$$

thus we can deduce the Debye-Waller factor B_T at temperature T.

The Chipman & Paskin formula [26] for the correction of the TDS from powdered crystals, Eq. (2.17):

$$\sigma = (\frac{\pi}{3})^{1/3} M_D \, a \, \Delta \frac{\cos\theta}{\lambda}$$

can be rewritten for the EDXD method as follows:

Δ is the width of the window of a given Bragg peak on the angular scale of 2θ for the ADXD method, we transform it into an energy scale:

$$\Delta = \arcsin(\frac{6.2}{d.E_r}) - \arcsin(\frac{6.2}{d.E_l}) ,$$

where E_r, E_l are in KeV and are equivalent to $(X + \delta)$ and $(X-\delta)$ [26] respectively and d is in Å. X is the position of the Bragg peak on the 2θ scale.

Therefore the TDS correction σ can be calculated from:

$$\sigma = (\frac{\pi}{3})^{1/3} M_D \, a \cos\theta \left\{\arcsin(\frac{6.2}{d.E_r}) - \arcsin(\frac{6.2}{d.E_l})\right\} \frac{E}{hc} . \qquad (3.8)$$

3.2 Instrumentation

The experimental set up consists of: an x-ray source, a specimen chamber, a detector and a multichannel analyzer. The schematic diagram showing the instrumental arrangement is in Fig. 3.1.

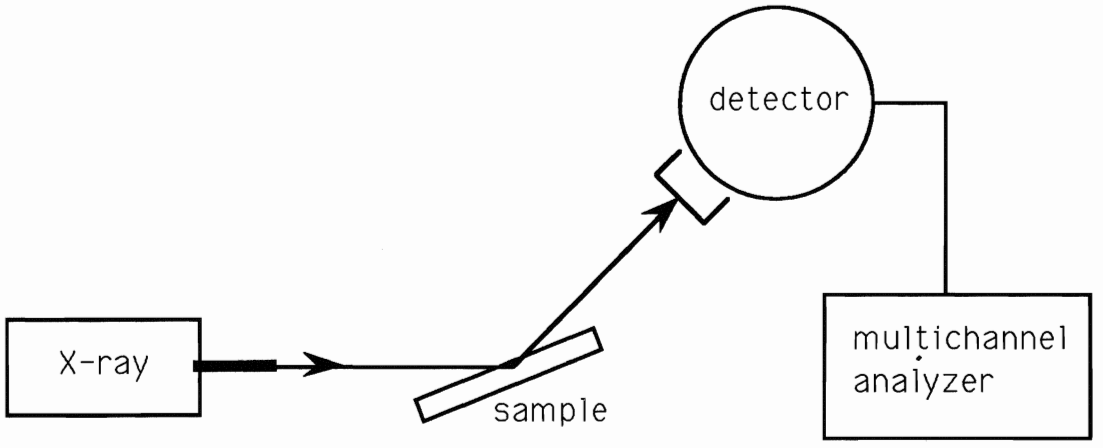

Fig 3.1 : The schematic diagram of the instrumental set up.

3.2.1 The x-ray source:

Continuous x-rays are produced when energetic electrons are rapidly decelerated upon collision with atoms of the x-ray tube anode. The kinetic energy of an electron on impact with the anode surface is:

$$K.E = eV = \frac{1}{2}mv^2,$$

where e, m, v are its charge, its mass and its velocity respectively, and V is the voltage of a x-ray tube.

When electrons strike the target, most of their kinetic energy is dissipated into heat, only a fraction of one percent is transformed into x-rays. Some electrons are stopped in one collision with the anode surface atoms, give up all energy at once and emit x-rays with the maximum possible energy E_{max}:

$$E_{max} = eV.$$

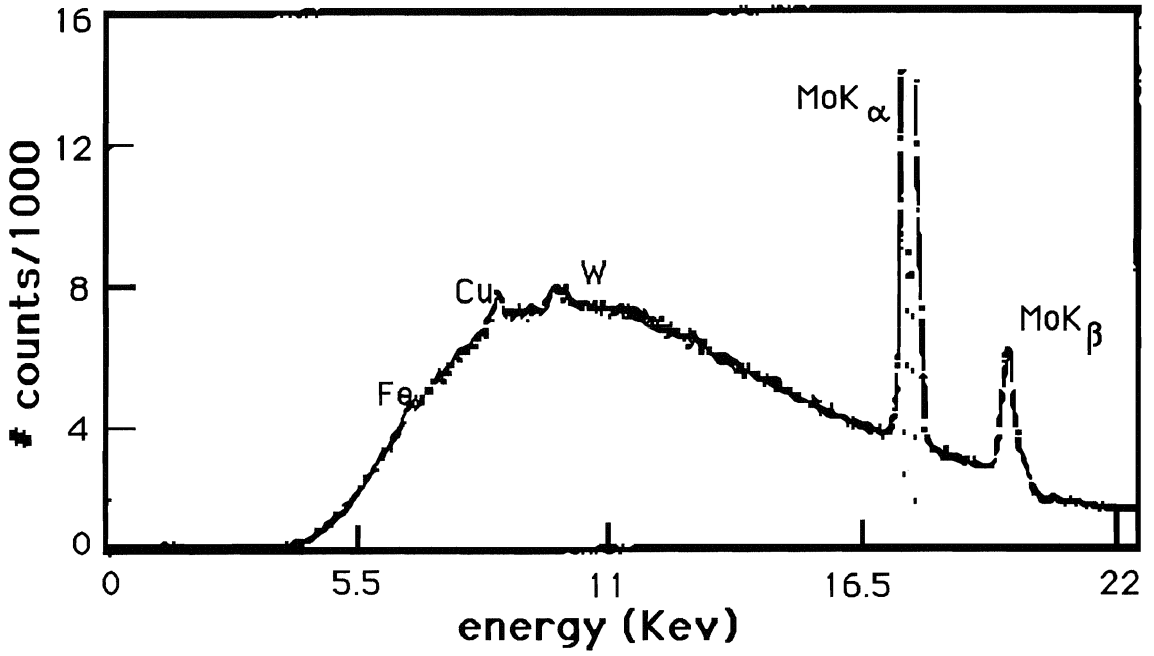

Fig. 3.2: The spectrum of x-ray radiation from a M_o tube operated at 30KeV and 1mA.

We have used a molybdenum x-ray tube. The maximum voltage is 60 KV and the maximum power is 2400W. We have operated at 30KV and 15mA. Fig. 3.2 shows the spectrum of the x-ray radiation at 30KV and 1mA. To record the spectrum of x-rays, we aimed the Si(Li) detector directly at the incident beam. The detector window was protected by a lead sheet so x-rays only reach the detector through a very small opening Because of a very high counting rate at the center of the x-ray beam which can over load the detector, we have set the opening slightly off the center of the beam. Therefore we could only record the spectrum near the edge of the x-ray beam. The radiation has been weakly contaminated with characteristic lines of Fe (6.403KeV), Cu (8.040KeV

and 8.970KeV) from the collimator and of W (9.671KeV) from the vaporization of the filament. There are two characteristic lines of M_oK_α and M_oK_β (17.441KeV and 19.605KeV).

3.2.2 The specimen chamber [4]:

The diagram of the specimen chamber is shown in Fig. 3.3a. A specimen is clamped down by two stainless steel clips on the surface of a copper block furnace which is heated by three heater cartridges (70Ω, 200W) inserted into the center of the copper block. They are electrically connected in parallel. The copper block is attached to the L- shape stainless steel shield which is mounted on a brass base by a ceramic rod, it can be rotated about a vertical axis so it can be set at any angle with respect to the incident x-ray beam. The brass base slides along the translation direction in the incident plane (Fig. 3.3b) on a brass slab which is mounted on the base of the vacuum chamber. The electric wires for the furnace and thermocouples are fed through the base. There are three thermocouples: one is connected to a heat supply- temperature controller, one gives temperature readings on the surface of the copper block, one reads the temperature on the surface of the specimen (we used a Pt thermometer in our experiment), they are clamped down to surfaces separately by stainless steel clips (Fig 3.3c). Thermocouples 1 and 2 should give the same reading. The chamber cover has three small entrance windows and one large exit window for x-rays, they form three angles of scattering: 26^0, 46^0 and 66^0. A vacuum pump is connected to the chamber through the openning from the base, it provides an inside pressure of about 25μm (to reduce air scattering and to prevent oxidization at high temperature).

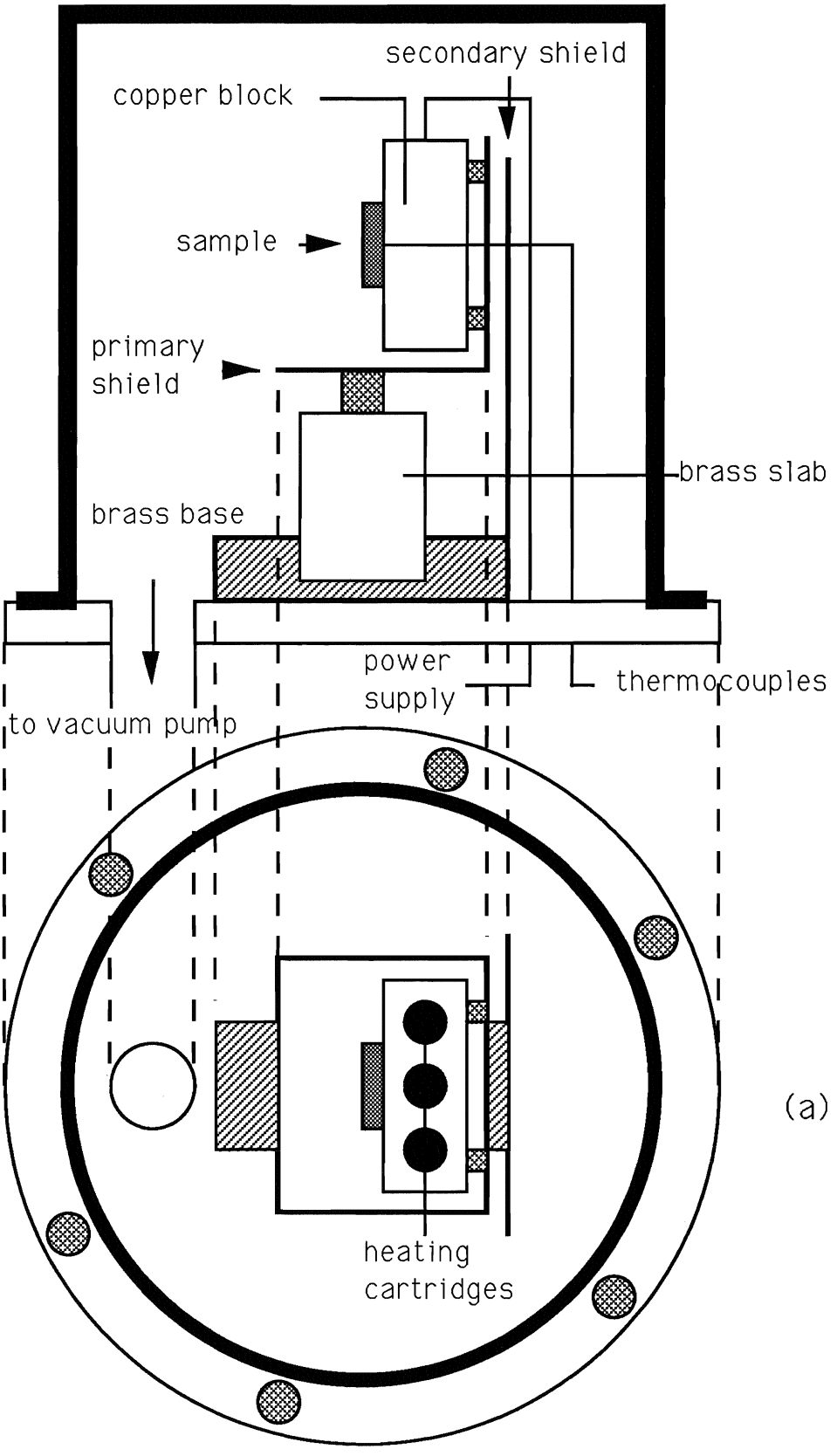
secondary shield
copper block
sample
primary
shield
brass slab
brass base
power
supply
thermocouples
to vacuum pump
heating
cartridges

(a)

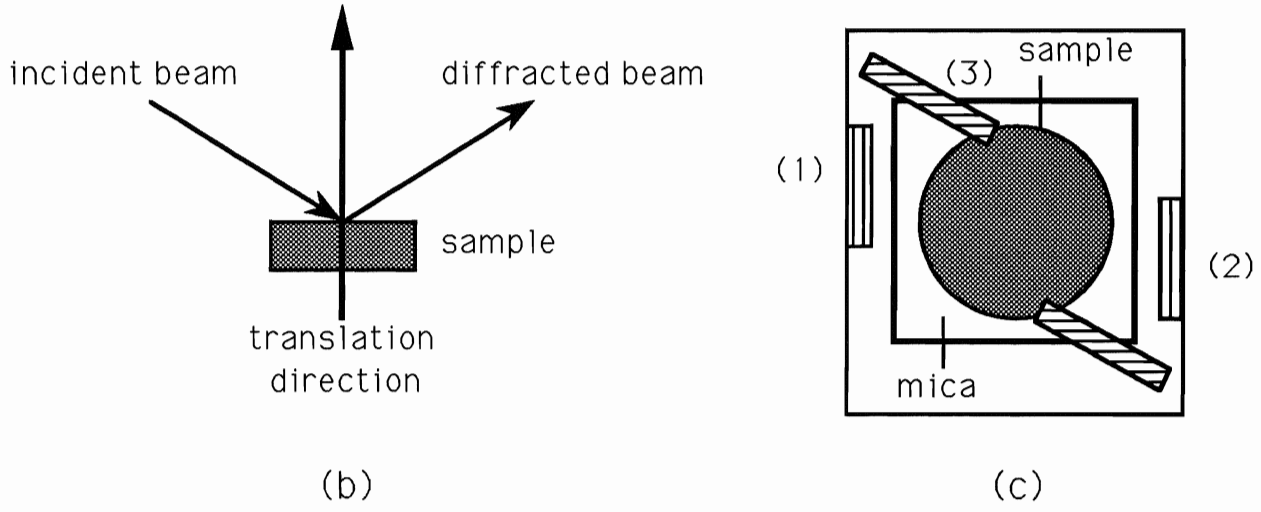

Fig. 3.3 (a) The specimen chamber (b) the translation direction of the sample, (c) the positions of three thermocouples.

3.2.3 The detector:

The depletion depth of a silicon diode detector is limited to 1-2mm. If a thicker depth is required, the process of lithium drifting can be applied to create a larger region, 5-10mm thick, of "intrinsic" Si in which the concentration of acceptors and donors are exactly balanced. This region can be used as an active volume of a detector. Such a detector is called a lithium-drifted silicon, Si(Li), detector. The detector is characterized by the detection efficiency (ε) and the energy resolution (R). ε is defined as:

$$\varepsilon = \frac{\text{number of full energy pulses recorded}}{\text{number of photons incident on the detector}}$$

and R is defined as the ratio of the full width at half maximum (FWHM) of the full energy peak corresponding to a monoenergetic x-ray over the

energy of the peak centroid. Our detector is Si(Li), model SPL-10180 by EG&G ORTEC. The beryllium window is 10mm in diameter and .025mm thick. The depletion depth is 5mm. The detection efficiency is 100% for radiation between 5KeV and 20KeV, the Be window absorbs lower energy radiation while Si becomes transparent to higher energy radiation. The energy resolution is about 180eV at 5.9KeV. Fig. 3.4 shows the measurement of the detector resolution by using a radioactive source of ^{55}Fe. The detector has been operated at liquid nitrogen temperature with a reverse bias voltage of 1200V.

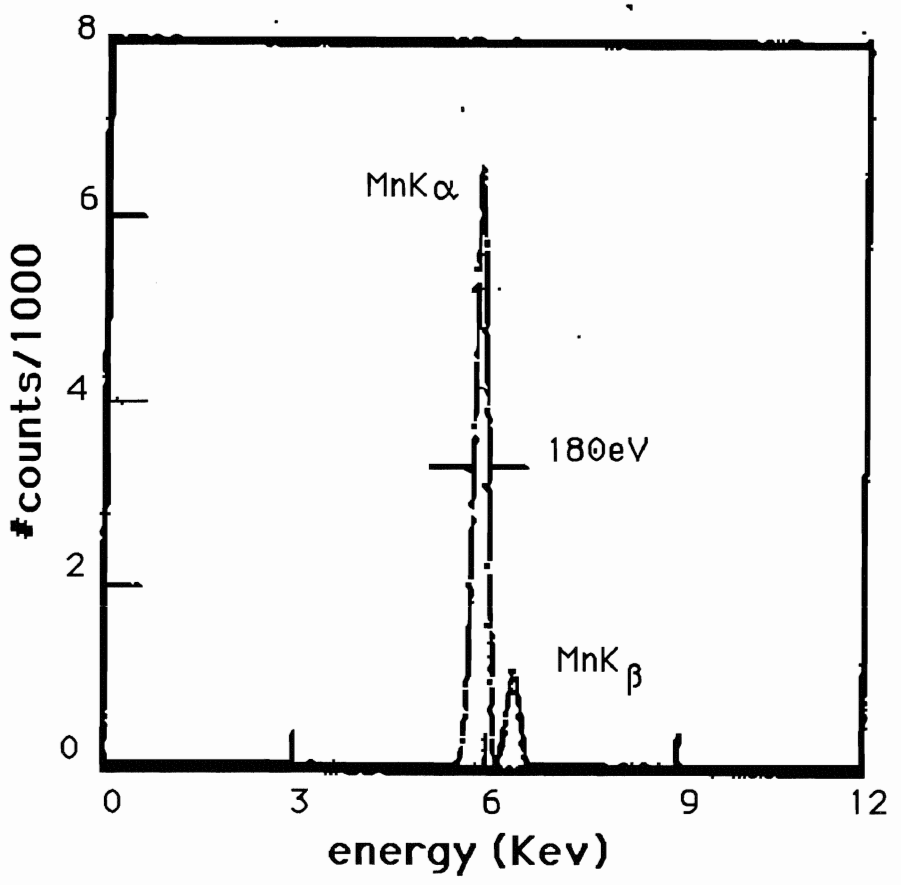

Fig. 3.4 The spectrum of the radioactive source of ^{55}Fe was used to measure the detector resolution.

3.2.4 The multichannel analyzer:

The multichannel analyzer (MCA) converts analog signals to equivalent digital numbers by an analog-to-digital converter (ADC) and stores them in the memory. Because components of an MCA are compatible with those of a standard personal computer (PC), plug-in-cards that convert a PC into an MCA are available. Our MCA is a personal computer analyzer (PCA) card, made by NUCLEUS, which can be installed in a full length slot of an IBM personal computer. The PCA card contains a100Hz Wilkinson ADC, a multichannel scaler and a dual port memory.

.

CHAPTER 4

EXPERIMENTAL DEVELOPMENT AND RESULTS

4.1 Determining intensity of a diffraction peak.

Fig. 4.1 shows an energy spectrum of x-rays scattered from a powder sample. It consists of diffraction peaks and characteristic x-ray peaks. To measure the intensity of a diffraction peak, the number of counts in the peak above the background is determined with reference to Fig. 4.2, which shows a diffraction peak in detail. The peak region is defined by the left (l_c) and right hand (r_c) channels. The computer calculates the average number of background counts per channel at l_c and r_c as follows:

$$L_c = < L_c+L_{c-1}+L_{c-2}+L_{c-3} >,$$

where L_c, L_{c-1}... are the number of counts in channels l_c, l_{c-1}...etc.

Similarly for R_c:

$$R_c= < R_c+R_{c+1}+R_{c+2}+R_{c+3} >.$$

The channel number of the centroid of the peak is calculated as follows:

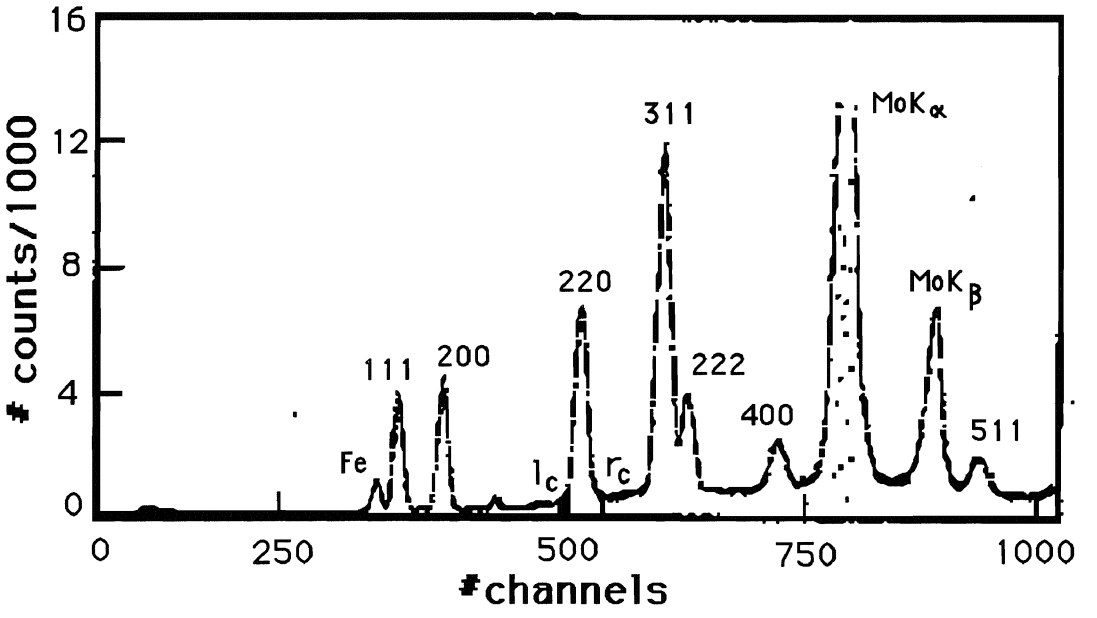

Fig. 4.1 Spectrum of an aluminum powder sample diffracted at the scattering angle of 46°.

$$CTRD = \frac{Y_1X_1+Y_2X_2+ \ldots\ldots+ Y_nX_n}{Y_1+Y_2+\ldots\ldots+Y_n},$$

where X is the channel number from the beginning of the diffraction peak and Y is the net counts in the channel X.

We can define:

T= the GROSS intensity is the total number of counts in the spectrum summed from channel l_c to channel r_c (the total area under the peak).

B= the BACKGROUND intensity is the number of count summed from channel l_c to channel r_c with an average background count per

channel equal to $(L_C + R_C)/2$

$$B = \frac{L_C+R_C}{2} (r_C - l_C + 1).$$

N= the NET intensity is the total number of counts in the diffraction peak:

$$N = T - B.$$

The gross intensity, the background intensity and the net intensity are shown in Table 4.1.

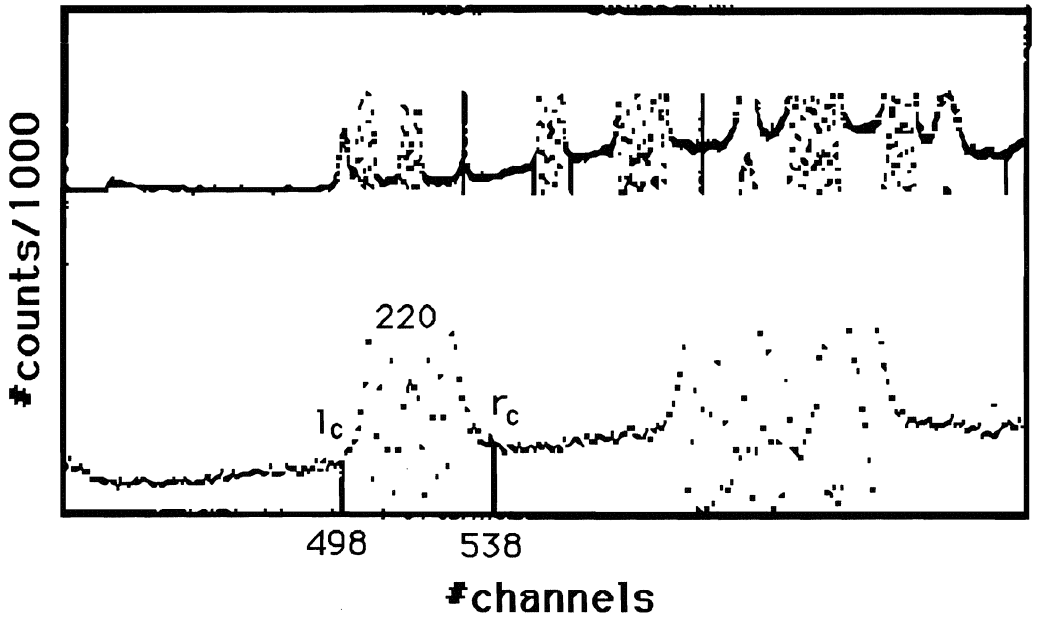

Fig. 4.2 The blow up of the spectrum in Fig. 4.1 for determining the intensity of the (220) peak. l_c is at channel 498, r_c is at channel 538.

The statistical error σ_N can be calculated as follows:

For the gross intensity:

$$\sigma_T = \sqrt{T}\,.$$

For the background intensity:

$$\sigma_B = \frac{\sigma_{L+R}}{2}(\,r_c - l_c + 1\,),$$

where $\frac{\sigma_{L+R}}{2}$ is the statistical error of each channel.

But $$\sigma_{L+R} = \sqrt{\sigma_L^2 + \sigma_R^2},$$

with $$\sigma_L = \frac{1}{2}\sqrt{L_c} \text{ and } \sigma_R = \frac{1}{2}\sqrt{R_c}\,.$$

So $$\sigma_N = \sqrt{\sigma_T^2 + \sigma_B^2}$$

and $$\%\sigma_N = 100\,\frac{\sigma_N}{N}\,.$$

The following definitions are used:

(i) The absolute intensity $I_T(hkl)$ of a diffraction peak (hkl) at temperature T equals the net intensity (N) recorded by the detector.

(ii) The relative intensity $\frac{I_T(hkl)}{I_T(h_ok_ol_o)}$ equals the ratio of the absolute intensity of a diffraction peak (hkl) to that of a peak $(h_ok_ol_o)$. $I_T(hkl)$ and $I_T(h_ok_ol_o)$ are recorded symultaneously at the same temperature T.

(iii) The relative intensity $\frac{I_R(hkl)}{I_T(hkl)}$ equals the ratio of the absolute intensity of a diffraction peak (hkl) at room temperature to that of the

same peak at temperature T. I_R(hkl) and I_T(hkl) are recorded sequentially at room temperature and at temperature T.

Table 4.1 Gross, background, net intensites from an aluminum spectrum for (220), (311+222) and (400) peaks. Unit of centroid in KeV.

PEAK	CTRD	GROSS	BCKGRD	NET
220	11.26	66846± 258	12956 ± 259	53890± 366
311+222	13.34	162833± 408	32045 ± 510	130788± 653
400	15.89	36748± 192	21774 ± 321	14974± 374

4.2 The stability of the incident beam and the reproducibility of absolute intensities at room temperature.

Elyaseery [4] reported that the intensity of the incident x-ray beam was not stable, therefore the intensities of the diffraction peaks were not consistent from one measurement run to the other on the same sample in the same geometrical condition.

We performed a series of measurements on a rotated unpressed aluminum powder sample at room temperature to check the reproducibility of intensity measurements. The system was carefully kept at the same condition for each run, except the x-ray generator was switched off and on between runs. The measurements were made over two days. During each measurement, the voltage and the current were carefully observed and adjusted if necessary to make sure that the x-ray generator was operating at 30KV and 15mA. The absolute intensities and the relative intensities, normalized to (220) lines of five diffraction peaks

are given in Table 4.2. The intensities were reproducible throughout the four measurements with a standard deviation of less than 3%. The result of the test measurements has demonstrated that the incident x-ray beam intensity was stable.

Table 4.2 Absolute and relative intensities of four measurements, the first line is the absolute intensity and the second line is the relative intensity with respect to line (220).

PEAK	RUN - 1	RUN - 2	RUN - 3	RUN - 4
111	4897 ± 118	4780 ± 119	4704 ± 121	4873 ± 119
	52.0 ± 1.8	51.4 ± 2.0	48.8 ± 2.0	50.6 ± 2.0
200	3993 ± 110	3994 ± 120	3985 ± 119	3878 ± 120
	42.4 ± 2.2	42.9 ± 1.9	41.3 ± 1.9	40.2 ± 1.8
220	9414 ± 141	9301 ± 139	9648 ± 145	9638 ± 143
	100	100	100	100
311+222	20615 ± 265	20768 ± 268	21411 ± 264	20978 ± 264
	219.0 ± 6.1	223.3 ± 6.2	221.9 ± 6.0	217.7 ± 5.9
400	2470 ± 150	2320 ± 139	2371 ± 142	2465 ± 149
	26.2 ± 2.0	24.9 ± 1.9	24.6 ± 1.8	25.6 ± 1.9

4.3 Intensities of diffraction lines as a function of temperature from unpressed samples.

A x-ray beam of 30KV, 15mA was used on an unpressed

aluminum powder sample (S-1) mounted inside a sample chamber [described in section 3.3.2], at an angle of 23° with respect to the direction of the incident beam.

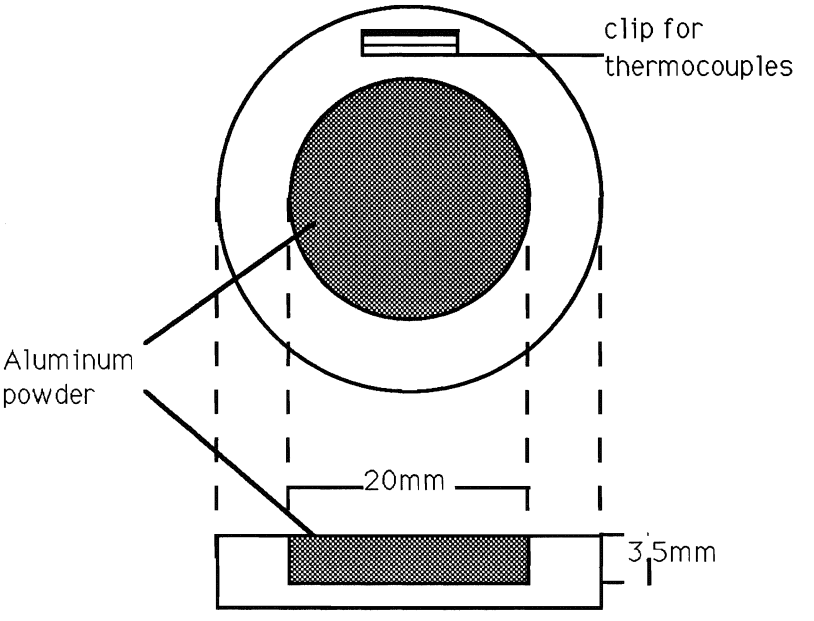

Fig. 4.3 A cavity type aluminum powder sample.

Diffracted beams were received by the detector through a slit of 1mm x 10mm. Aluminum powder, supplied by Fisher Scientific was hand sieved through a 400 mesh and was packed into a cavity type sample holder of 20mm in diameter and of 3.5mm thick made of copper (Fig. 4.3). The sample holder was mounted on the surface of a copper block furnace. Two thermocouples (one was connected to a heat supply-temperature controller, one was connected to a voltmeter to give a second reading, both should give the same temperature) were attached to the front edge of the sample holder by a small stainless steel clip.The density of unpressed samples was about 40% to 50% of that of aluminum solid. The reason for our choice of the power of the x-ray beam and the angle of incidence was that we thought we would see the highest number of

diffraction lines of aluminum powder: six lines from (111) to (511) with two lines (331+420) and (422) missing because they overlaped with MoK_α and MoK_β lines.We firstly measured the intensities of the diffraction lines at room temperature and subsequently measured at four higher temperatures of 382K, 490K, 586K and 689K. We calculated the relative intensity $\frac{I_R(hkl)}{I_T(hkl)}$ for each line. ln (I_R/I_T) versus $1/(4d_R^2)$ is plotted in Fig. 4.4 in accordance with Eq. (3.6). Values of $\ln(I_R/I_T)$ for four temperatures are given in Table 4.3.

We repeated the measurements on a different unpressed aluminum sample (S-2) with a geometrical condition as close as before, at room temperature and four others at 375K,498K,592K and 701K. We could not select the previous temperatures exactly because temperature readings fluctuated. A set of similar results are tabulated in Table 4.4 and plotted in Fig.4.5.

The values of ln (I_R/I_T) and (I_R/I_T) of each set of measurements from Tables 4.3 and 4.4 show no significant increase with $1/(4d_R^2)$ from (111) to (311+222). The overall results in Table 4.4 seem to be systematically higher than those in Table 4.3. The lack of reproducibility in the ratio (I_R/I_T) is evident in many cases.

We suspected that the problem of non-linearity of ln (I_R/I_T) and the lack of reproducibility of the two sets of measurement were related to the large grain size and loose packing of the aluminum powder. Any change in the mechanical condition of the sample (a change in the orientation of the large grains) or any small change in the geometry of the system

during the heating/cooling cycle could probably induce a significant affect on the absolute intensities of the diffracted beams.

Table 4.3 Values of ln (I_R/I_T) (first line) and (I_R/I_T) (second line) of the sample (S-1) at four different tempeartures (K).

PEAK	382	490	586	689	$1/4d_R^2$
111	.02 ± .02	.05 ± .02	.18 ± .02	.32 ± .03	.046
	1.02 ± .02	1.06 ± .02	1.19 ± .02	1.37 ± .04	
200	.07 ± .02	.11 ± .02	.27 ± .02	.39 ± .02	.061
	1.07 ± .02	1.12 ± .02	1.31 ± .03	1.47 ± .03	
220	.05 ± .02	.16 ± .02	.13 ± .02	.37 ± .02	.122
	1.05 ± .02	1.18 ± .02	1.14 ± .03	1.44 ± .03	
311+222	.04 ± .01	.16 ± .01	.28 ± .01	.43 ± .02	.175
	1.04 ± .01	1.18 ± .01	1.32 ± .01	1.52 ± .03	
400	.09 ± .08	.35 ± .08	.54 ± .11	.68 ± .12	.244
	1.10 ± .09	1.42 ± .11	1.72 ± .19	1.98 ± .24	
511	.22 ± .09	.53 ± .11	.79 ± .13	1.13 ± .17	.412
	1.24 ± .11	1.71 ± .19	2.20 ± .29	3.89 ± .66	

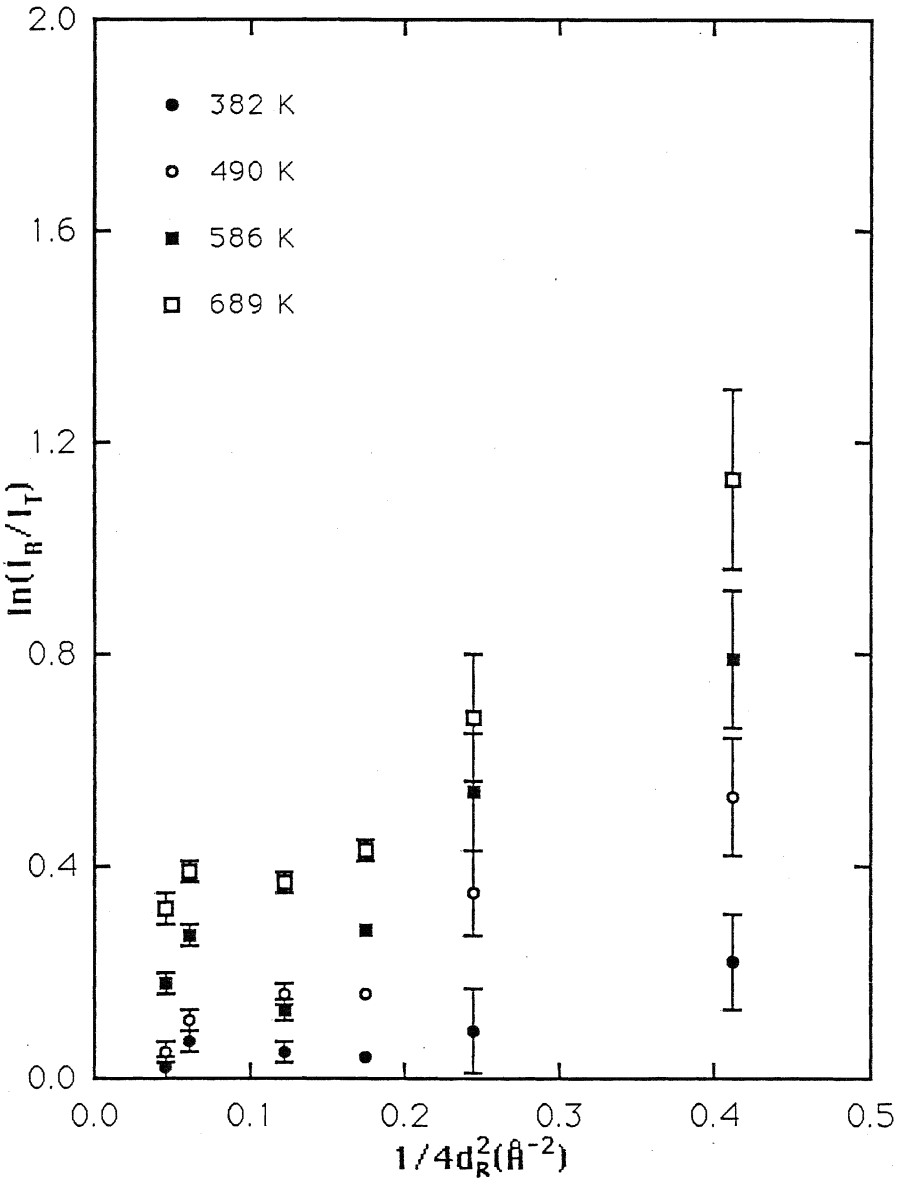

Fig 4.4 The Wilson plot of ln (I_R/I_T) versus $1/(4d_R^2)$ for the sample (S-1).

Table 4.4 Values of ln (I_R/I_T) (first line) and (I_R/I_T) (second line) of the sample (S-2) at four different tempeartures (K).

PEAK	375	498	592	701	$1/d_R^2$
111	.08 ± .02	.25 ± .03	.43 ± .03	.50 ± .03	.046
	1.09 ± .02	1.29 ± .04	1.54 ± .05	1.65 ± .05	
200	.10 ± .02	.25 ± .03	.38 ± .03	.44 ± .03	.061
	1.10 ± .02	1.28 ± .04	1.46 ± .04	1.56 ± .05	
220	.07 ± .02	.20 ± .02	.34 ± .02	.42 ± .02	.122
	1.07 ± .02	1.23 ± .02	1.41 ± .03	1.53 ± .03	
311+222	.09 ± .02	.27 ± .02	.41 ± .02	.53 ± .02	.175
	1.09 ± .02	1.30 ± .03	1.50 ± .03	1.71 ± .03	
400	.14 ± .10	.32 ± .12	.53 ± .12	.64 ± .13	.244
	1.15 ± .11	1.37 ± .16	1.69 ± .20	1.89 ± .24	
511	. 17 ± .09	.57 ± .11	1.05 ± .16	1.33 ± .20	.412
	1.19 ± .11	1.77 ± .19	2.86 ± .46	3.80 ± .76	

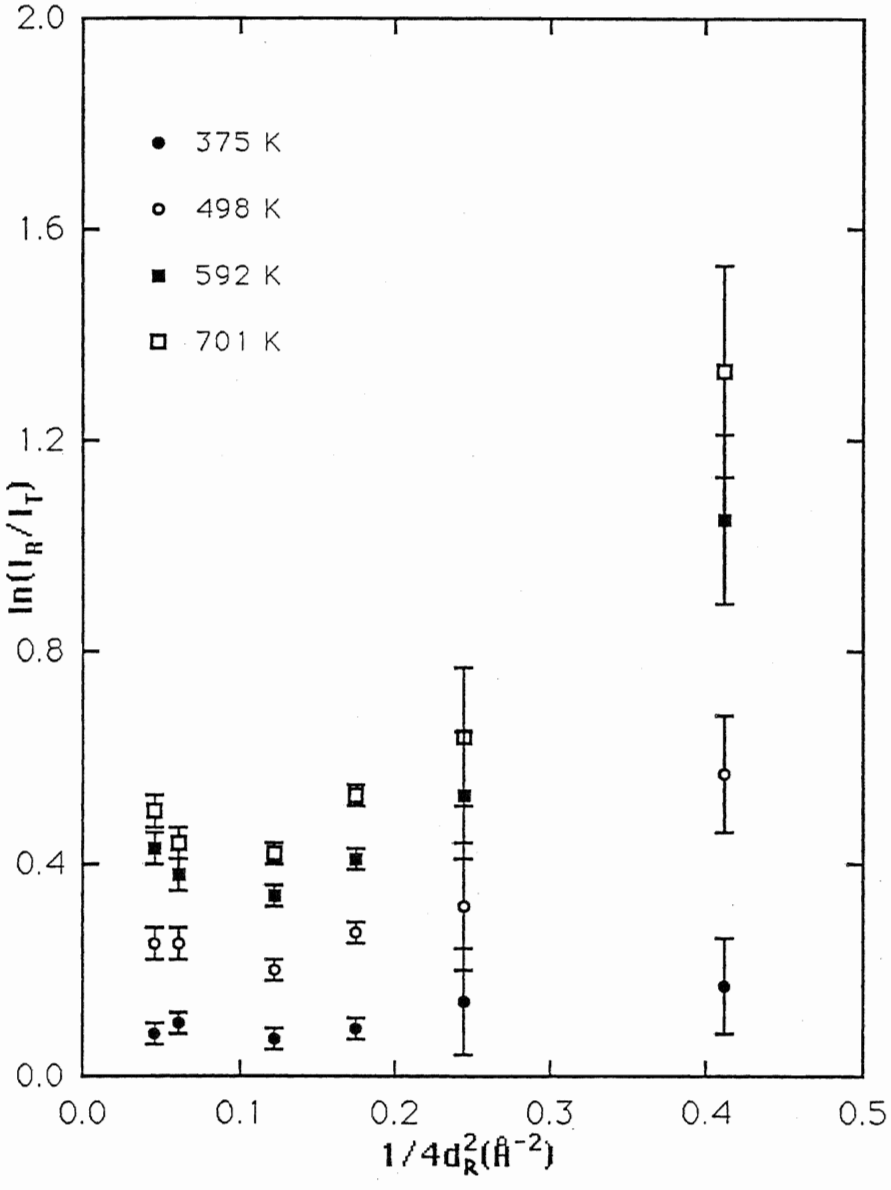

Fig 4.5 The Wilson plot of ln (I_R/I_T) versus $1/(4d_R^2)$ for the sample (S-2).

To illustrate the sensitivity of the absolute intensity measurements to small geometry (or sample) changes. We performed two intensity measurements on an unpressed aluminum powder sample with identical conditions except the position of the detector slit was changed by 2mm. The distance between the sample to the detector is about 120mm, so the difference of 2mm corresponds to about 1^{o} change in the scattering angle. Table 4.5 gives the absolute intensities of the two measurements and the intensity ratios. The relative intensity of (111) and (220) shows a 35% difference between the two measurements.

From Table 4.5, we conclude that the condition for the reproducibility of the intensity measurements was that there should be no change in geometry or powder sample grain structure during heating and cooling.

Table 4.5 Comparison of absolute intensities of two measurements with different slit positions.

PEAK	EXPRMT - 1	EXPRMT - 2	RATIO
111	4232 ± 94	3625 ± 97	1.17 ± .06
200	6728 ± 118	6467 ± 119	1.04 ± .04
220	17529 ± 228	20308 ± 206	.86 ± .02
311+222	41768 ± 377	44295 ± 402	.94 ± .02

4.4 Some modifications to the powder sample, temperature measurements and the detection geometry.

The reproducibility of the intensities of the diffraction lines required that the geometry of the experimental set up and the mechanical condition of the sample should not be disturbed. In an unpressed sample, aluminum powder was loose packed into a sample holder cavity. Its density was only about 40% to 50% of that of aluminum solid. At high temperature, crytals could possibly move about because there was a large volume of empty space around them. When a sample was brought back to room temperature, crystals did not necessarily orient to the same directions as before, thus it was possible that a new intensity measurement could not reproduce the same result. We thought that this effect may be reduced if we pressed aluminum powder into a tablet because the grains could not so easily move at high temperature, so the orientation of the grains may be the same after a temperature cycle. Moreover, using a pressed powder tablet, the temperature on the surface of the sample could be measured.This could not be easily done with an unpressed sample. We decided to make a new sample by pressing aluminum powder into a tablet of 13.6mm in diameter and 3.5mm thick. We clamped the sample on the surface of the copper block by two stainless steel clips. We separated interfaces of the tablet and the block by a thin sheet of mica to prevent a phase change at the interface during intensity measurements at high temperature because aluminum and copper interact around 800K [see Fig. 3.3.c].

We had been using an 1mm slit in front of the detector. A wider

slit would increase the number of diffracting grains seen by the detector, so effectively it would reduce the intensity changes due to the grain size effect. It also increased the intensity of diffraction lines, effectively it decreased the statistical error and the running time. To check if the intensity to background ratio would be effected by a wider slit, we did a test by measuring the intensities of (220) and (400) diffraction lines with a 3mm slit and compared it to that of a measurement made with a 1mm slit. The comparison of two runs showed that the signal to noise ratio did not change significantly. The result was given in Table 4.6.

Table4.6 Comparison of the signal to noise ratio of 1mm slit and 3mm slit.

PEAK	3mm SLIT			1mm SLIT		
	NET CNT	BCKGND	SGNL/NSE	NET CNT	BCKGND	SGNL/NSE
220	25146±233	4992 ± 156	5.04 ±.20	13056±164	2618 ± 105	4.99 ±.26
400	5233 ±228	8132 ± 196	.64 ±.04	2656±140	3780 ± 115	.70 ± .06

For temperature readings, we used two thermocouples and a platinum thermometer. Two thermocouples were attached separately on the surface of the copper block by two small stainless steel clips as shown in Fig. 3.3c: thermocouple (1) was connected to a heat supply - temperature controller, thermocouple (2) gave temperature readings at the surface of the copper block. A Pt thermometer was mobile. We did three temperature measurements for a testing purpose:

(i) test 1: Pt thermometer was directly attached on the surface of the copper block to check the variation of its temperature readings with

that of thermocouple (2) (Table 4.7.a).

(ii) test 2: same as test 1 but Pt thermometer was separated from the surface of the copper block by a thin sheet of mica, so temperature readings were the same as that of the bottom of the sample (Table 4.7.b).

(iii) test 3: Pt thermometer was attached to the surface of the sample (Table 4.7.c) to give temperature readings of the surface of the sample.

Table 4.7.a Test 1: comparison of temperature readings of Pt thermometer and thermocouple (2), in (^{0}C).

THERMCPL(2)	Pt THERMMTR	DIFFERENCE
22.0 ± .1	22.0 ± .1	0.0 ± .2
132.0 ± .7	131.0 ± .8	1.0 ± 1.4
253.0 ± 1.3	252.0 ± 1.5	1.0 ± 2.8
371.0 ± 1.8	369.0 ± 2.2	2.0 ± 4.1
499.0 ± 2.5	496.0 ± 3.0	3.0 ± 5.5
628.0 ± 3.1	622.0 ± 3.7	6.0 ± 6.7

Table 4.7.a shows that the variation of temperature readings from a thermocouple and from a platinum thermometer was 1^{0}C at 132^{0}C and increased to 6^{0}C at 628^{0}C, it might due to the way we clamped the Pt thermometer onto the surface of the copper block so it did not have a very good contact. Table 4.7.b shows that a thin sheet of mica could significantly reduce the temperature of the sample at high temperature (reduced by 37^{0}C at 592^{0}C). Table 4.7.c shows the temperature gradient

from the bottom to the top of the sample was only 9^0C at 592^0C, which was insignificant in the measurement of the Debye-Waller factor of aluminum at that temperature.

We did two test runs with the same pressed sample, one before and one after a temperature cycle. The angle of diffraction was 46^o, a 3mm slit was placed in front of the detector. We measured the intensities of (220), (311+222) and (400) lines. It has been clearly demonstrated that the reproducibility could be achieved if a pressed sample of aluminum powder was used to scatter a stable x-ray radiation with a 3mm slit placed in front of the detector. The results is shown in Table 4.8.

Table 4.7.b Test 2:temperature readings at the bottom of the sample (^{0}C).

THERMCPL(2)	PtTHERMMTR	DIFFERENCE
22.0 ± .1	22.0 ± .1	0.0 ± .2
142.0 ± .7	137.0 ± .8	5.0 ± 1.5
264.0 ± 1.3	252.0 ± 1.5	12.0 ± 2.8
373.0 ± 1.9	352.0 ±.2.1	21.0 ± 4.0
491.0 ± 2.4	463.0 ± 2.8	28.0 ± 5.2
592.0 ± 3.0	555.0 ± 3.3	37.0 ± 6.3

Table4.7.c Test 3: temperature reading at the surface of the sample(^{0}C).

THERMCPL(2)	PtTHERMMTR	VARIATION
22.0 ± .1	22.0 ± .1	0.0 ± .2
142.0 ± .7	137.0 ± .8	5.0 ± 1.5
264.0 ± 1.3	253.0 ± 1.5	11.0 ± 2.8
373.0 ± 1.9	355.0 ± 2.1	18.0 ± 4.0
491.0 ± 2.4	458.0 ± 2.7	33.0 ± 5.2
592.0 ± 3.0	546.0 ± 3.3	46.0 ± 6.2

Table 4.8 The result of two test runs for the reproducibility of the intensity measurements on a pressed sample, before and after a temperature cycle, with a 3mm slit.

PEAK	ABSL.INT.(R-1)	ASBL.INT (R-2)	RATIO
220	44681 ± 313	42131 ± 337	1.06 ± .02
311+222	92495 ± 555	94320 ± 566	.98 ± .01
400	11105 ± 344	10541 ± 337	1.05 ± .07

4.5 Determination of the variation of the Debye-Waller factor of aluminum with temperature.

An incident x-ray beam of 30KV, 15mA has been diffracted from a pressed aluminum powder sample. Diffracted beams were received by a detector through a 3mm slit . Three different angles of diffraction of 26^o,

46° and 66° were used to cover eight diffraction lines from (111) to (511), because only a portion of incident beam from 10.5KeV to 16.5KeV has been used in these measurements. There were two reasons for using this portion: with reference to Fig. 3.2 page 29, (a) the incident beam in this region was free from characteristic lines; (b) the intensity decreased slowly with energy so the intensity per unit energy, I(E), in a given diffraction peak varied only slightly with temperature,thus when we calculated the relative intensity (I_R/I_T) of the same diffraction line at different temperatures,.I(E) cancels out. Fig. 4.6 shows spectra taken at the three angles:

(a) angle of 26° shows two lines of (111) and (200),

(b) angle of 46° shows three lines of (220), (311+222) and (400),

(c) angle of 66° shows four lines of (400), (331+420), (422) and (511).

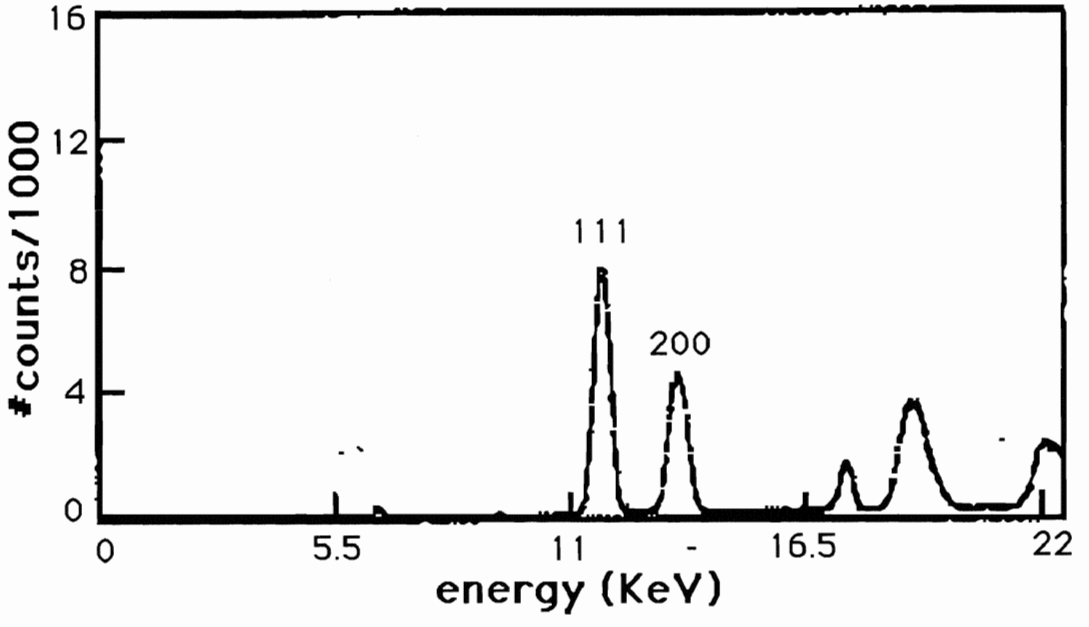

(a)

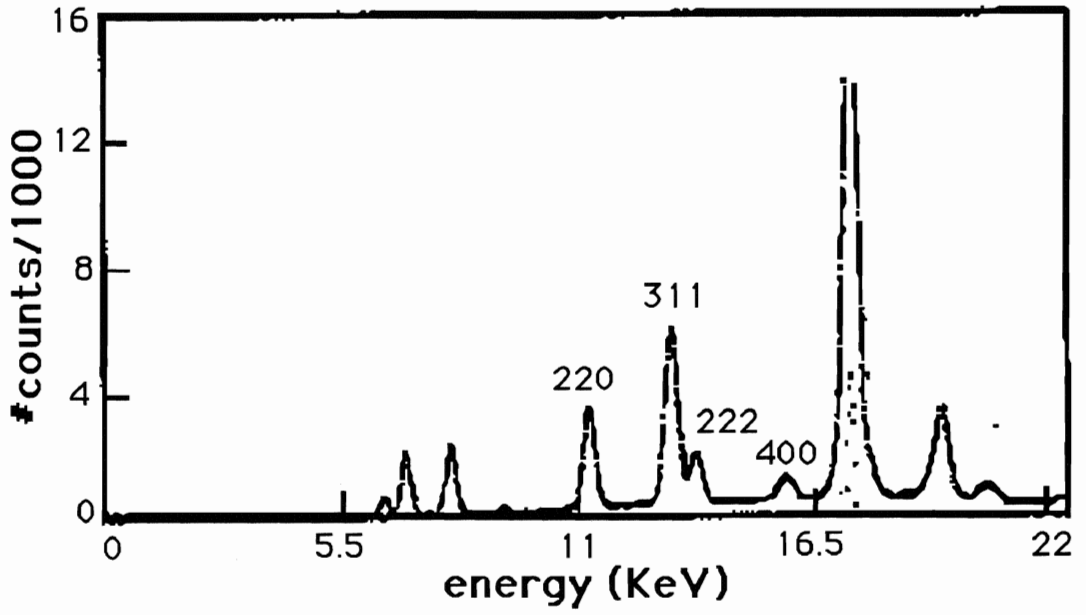

(b)

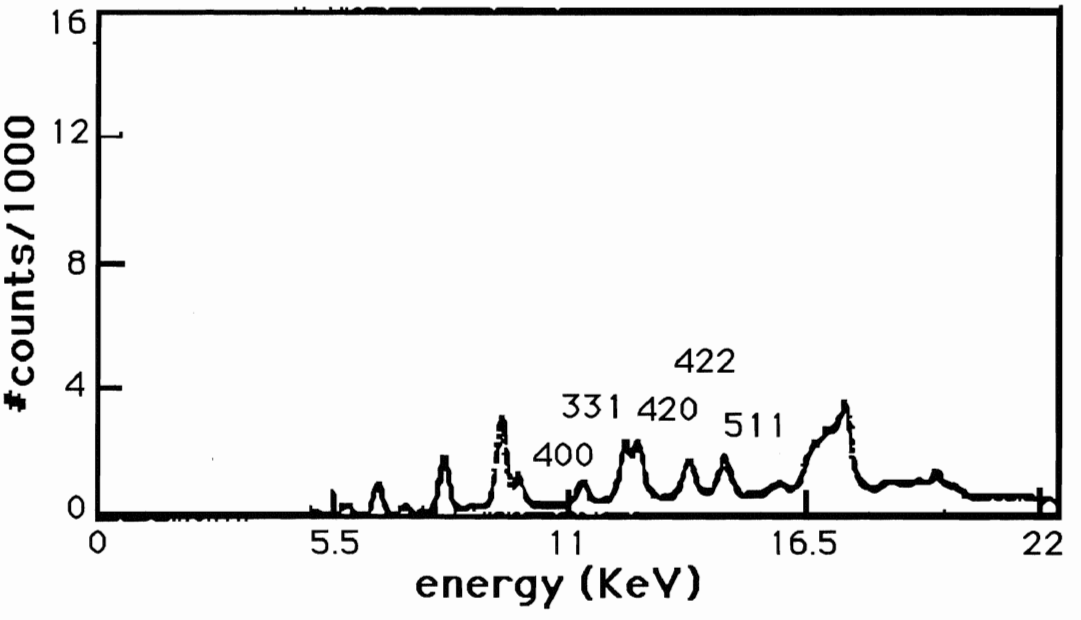

(c)

Fig. 4.6 Spectra of three angles of diffraction: (a) 26°, (b) 46°, and (c) 66°.

Table4.9 Absolute values of the intensities of eight diffraction lines at room temperature before (RUN-1) and after a temperature cycle (RUN-2) for three angles of diffraction.

PEAK	2θ(°)	RUN-1	RUN-2	RATIO
111	26	181741 ± 545	183210 ± 550	.99 ± .01
200		114002 ± 456	115153 ± 461	.99 ± .01
220	46	53239 ± 373	51904 ± 363	1.03 ± .01
311+222		127194 ± 636	127199 ± 636	1.00 ± .01
400		14640 ± 366	15245 ± 351	.96 ± .04
400	66	9098 ± 246	9426 ± 245	.97 ± .05
331+420		49892 ± 499	50447 ± 504	.99 ± .02
422		16871 ± 371	16577 ± 381	1.02 ± .04
511		17596 ± 369	17721 ± 372	. 99 ± .04

Intensities of eight diffraction lines have been measured at room temperature and subsequently at 410K,525K, 625K, 725K, and 815K. The running time depended on the intensity of the diffracted beam which was in turn dependant on the angle of diffraction: a smaller angle, a stronger diffracted beam, a shorter running time. Depending on the running time, each set of measurements at six different temperatures could be completed in one or two days. If two days were needed, we started a measurement at room temperature then at 410K,52K, 625K in the first day. We let the sample cool down overnight, on the second day

we started again at room temperature then at 725K, 815K.

Table 4.10.a Values of (I_R/I_T) for the first run.

		TEMPERATURE(K)				
PEAK	2θ(°)	410	525	625	725	815
111	26	1.07 ± .01	1.12 ± .01	1.19 ± .01	1.28 ± .01	1.35 ± .01
200		1.08 ± .01	1.15 ± .01	1.20 ± .01	1.32 ± .01	1.45 ± .01
220	46	1.09 ± .02	1.22 ± .02	1.35 ± .03	1.50 ± .03	1.79 ± .04
311+222		1.15 ± .01	1.30 ± .01	1.51 ± .02	1.74 ± .03	2.05 ± .04
400		1.27 ± .07	1.53 ± .09	1.78 ± .12	2.27 ± .18	2.72 ± .25
400	66	1.27 ± .08	1.55 ± .11	1.87 ± .17	2.88 ± .33	3.32 ± .38
331+420		1.23 ± .03	1.60 ± .04	1.98 ± .05	2.85 ± .10	3.86 ± .17
422		1.33 ± .07	1.80 ± .11	2.57 ± .19	3.63 ± .36	4.40 ± .54
511		1.36 ± .07	1.97 ± .12	2.90 ± .22	4.20 ± .42	6.07 ± .87

We repeated each set of measurements to see if it could be reproduced, it showed that this was the case for all temperatures. Table 4.9 shows the reproducibility of the intensity measurements of the diffraction lines at room temperature after a heating/cooling cycle for all three angles of diffraction. Table 4.10 shows the values of (I_R/I_T) for the run-1 (a), for the run-2 (b), and the average values of two runs (c).

Table 4.10.b Values of (I_R/I_T) for the second run.

		TEMPERATURE(K)				
PEAK	2θ(°)	410	525	625	725	815
111	26	1.06 ± .01	1.13 ± .01	1.18 ± .01	1.26 ± .01	1.32 ± .01
200		1.06 ± .01	1.14 ± .01	1.20 ± .01	1.31 ± .01	1.40 ± .01
220	46	1.11 ± .02	1.24 ± .02	1.38 ± .02	1.57 ± .03	1.83 ± .04
311+222		1.14 ± .01	1.34 ± .02	1.53 ± .02	1.82 ± .03	2.12 ± .04
400		1.24 ± .07	1.53 ± .09	1.74 ± .12	2.57 ± .23	3.12 ± .30
400	66	1.28 ± .07	1.62 ± .11	1.98 ± .16	2.66 ± .27	3.44 ± .44
331+420		1.26 ± .03	1.64 ± .03	2.03 ± .04	2.74 ± .09	3.93 ± .12
422		1.29 ± .06	1.84 ± .11	2.50 ± .18	3.68 ± .39	4.51 ± .54
511		1.39 ± .06	2.05 ± 12	3.05 ± .16	4.36 ± .30	5.83 ± .77

We corrected the absolute intensities for TDS, which varied from less than 1% for the (111) line at room temperature to 15% for the line (511) at 815K. The calculation for TDS corrections have been done by using Eq. (3.8):

$$\sigma = (\frac{\pi}{3})^{1/3} M_D \, a \cos\theta \left\{ \arcsin(\frac{6.2}{d\, E_r}) - \arcsin(\frac{6.2}{d\, E_l}) \right\} \frac{E}{hc} \, .$$

The lattice constant , a, was calculated by using the thermal expansion coefficient for aluminum [27]. A theoretical value was used for the Debye-Waller factor, M_D [5]. The remaining parameters were measured

experimentally. We took the average values of the relative intensities $I_R(hkl)/I_T(hkl)$ for all eight diffraction lines. We calculated ln (I_R/I_T) and used the Wilson plot, showed in Fig. 4.7, to determine the change in the Debye-Waller factor ΔB as a function of temperature. Table 4.11 shows:

(a)The values of ln (I_R/I_T) for five temperatures above room temperature and values of $(1/4d_R^2)$ of each diffraction line, and

(b) The corresponding values of slopes, intercepts and ΔBs.

Table 4.10.c Average values of (I_R/I_T) of two runs.

	TEMPERATURE (K)				
PEAK	410	525	625	725	815
111	1.06 ± .01	1.12 ± .01	1.18 ± .01	1.27 ± .01	1.34 ± .01
200	1.07 ± .01	1.14 ± .01	1.20 ± .01	1.31 ± .01	1.42 ± .01
220	1.10 ± .01	1.23 ± .01	1.36 ± .02	1.53 ± .02	1.81 ± .03
311+222	1.14 ± .01	1.32 ± .01	1.52 ± .01	1.78 ± .02	2.08 ± .03
400*	1.26 ± .03	1.56 ± .05	1.84 ± .07	2.74 ± .13	3.14 ± .17
331+420	1.24 ± .02	1.66 ± .04	2.00 ± .04	2.80 ± .07	3.89 ± .12
422	1.31 ± .05	1.82 ± .08	2.53 ± .13	3.65 ± .26	4.45 ± .38
511	1.37 ± .05	2.01 ± .08	2.98 ± .14	4.28 ± .26	5.95 ± .58

* Values of (400) line is the average of four values instead of two as the others.

Table 4.11.a Values of ln (I_R/I_T) and values of $1/4d_R^2$ ($Å^{-2}$) for five temperatures above room temperature.

	TEMPERATURE (K)					
PEAK	410	525	625	725	815	$1/4d_R^2$
111	.06 ± .01	.11 ± .01	.17 ± .01	.24 ± .01	.29 ± .01	.046
200	.07 ± .01	.13 ± .01	.19 ± .01	.27 ± .01	.35 ± .01	.061
220	.10 ± .01	.21 ± .01	.31 ± .01	.42 ± .01	.58 ± .02	.122
311+222	.13 ± .01	.28 ± .01	.42 ± .01	.58 ± .01	.73 ± .01	.175
400	.23 ± .02	.44 ± .03	.61 ± .04	.95 ± .05	1.15 ± .05	.244
331+420	.22 ± .02	.48 ± .02	.69 ± .02	1.03 ± .02	1.36 ± .03	.297
422	.27 ± .04	.60 ± .04	.93 ± .05	1.30 ± .07	1.49 ± .08	.366
511	.32 ± .04	.70 ± .04	1.09 ± .05	1.45 ± .06	1.78 ± .10	.412

Table 4.11b Values of slopes, intercepts and ΔBs for five temperatures above room temperature.

TEMP(K)	410	525	625	725	815
SLOPE	.70 ± .05	1.59 ± .05	2.46 ± .11	3.39 ± .13	4.04 ± 17
INTRCPT	.02 ± .01	.02 ± .01	.02 ± .03	.05 ± .03	.10 ± .04
$\Delta B_{(T)}(Å^2)$	.36 ± .03	.81 ± .03	1.27 ± .06	1.76 ± .07	2.11 ± .09

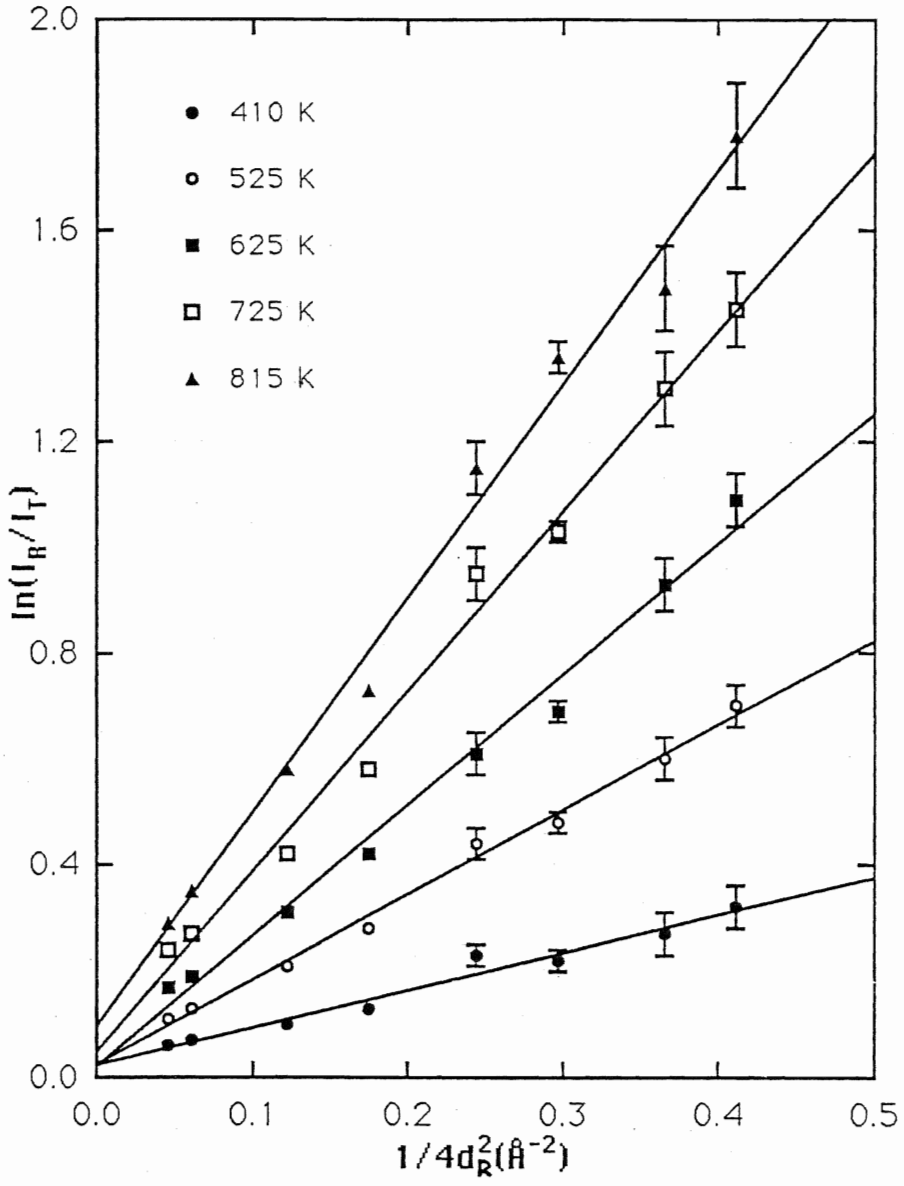

Fig. 4.7 The Wilson plot of $\ln(I_R/I_T)$ versus $(1/4d_R^2)$ for five temperatures.

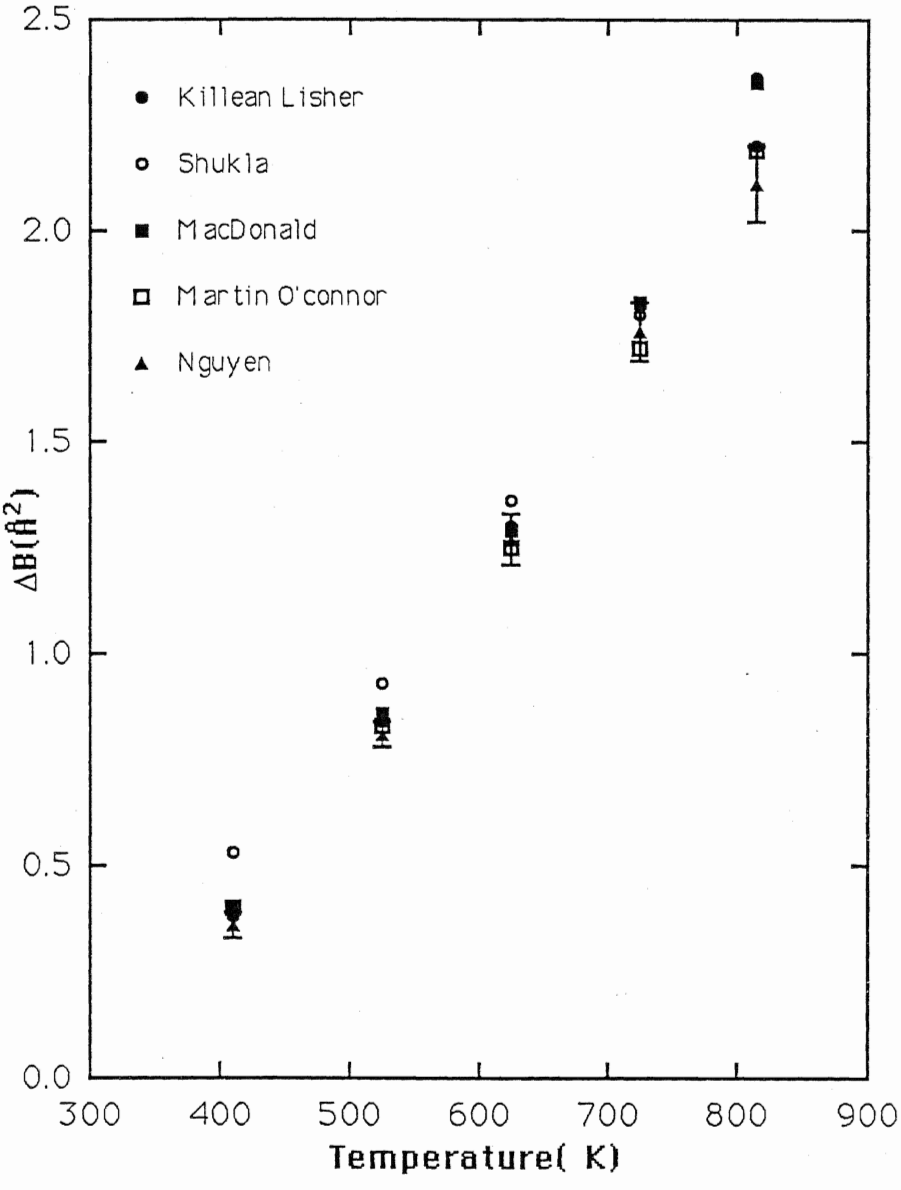

Fig 4.8 The plot of the comparison of our result with the others.

We conclude this chapter by comparing our result with two theoretical calculations from Killean & Lisher [5] and from Shukla [6], two experimental data from MacDonald [11] using the neutron diffraction method and from Martin & O' Connor [12] using the Mössbauer effect on single crytals. The comparison is given in Table 4.12, an asterisk (*) indicates theoretical calculation, our result is indicated by 'Nguyen'. The plots are given in Fig.4.8.

Table 4.12 The comparison of our result with that of Killean & Lisher (K&L), of Shukla, of MacDonald (M.D) and of Martin & O' Connor (M&O). Values in $Å^2$.

TEMP(K)	410	525	625	725	815
K&L*	.38	.84	1.30	1.82	2.36
SHUKLA*	.53	.93	1.36	1.80	2.20
M.D	.40	.86	1.29	1.83	2.35
M&O	.40	.83	1.25	1.72	2.19
NGUYEN	.36 ± .03	.81 ± .03	1.27 ± .06	1.76 ± .07	2.11 ± .09

CHAPTER 5

CONCLUSION

We have measured the change of the Debye-Waller factor from room temperature up to 815K for aluminum by using the EDXD system at Brock University. Our results were in good agreement with those previously measured by MacDonald [11] using neutron diffraction and by Martin & O'Connor [12] using Mössbauer spectroscopy on single crystals. Referring to Table 4.12, our values of the change of the Debye-Waller factor from room temperature were very close to that of Martin & O'Connor. The differences were about 2% at 525K, 62K, 725K and about 4% at 815K. The results from MacDonald were slightly higher in the temperature range from 525Kto 725K, but our results only differred by 2% to 6%. Since our experimental errors were from 4% to 5% in this temperature range, we could see that our results were well matched with his. At 815K, MacDonald's value was 11% higher than ours and 7% higher than that of Martin & O'Connor. At 410K, our result was 10% less than theirs but our error was 8%, so our result was still good. When we compared our results with that of Dingle & Medlin [10] from x-ray diffraction on a single crystal we got the same value of $\Delta B_{(T)}$ at 410^0K, and about 1% different at 525K. We did not put their results [10] in Table 4.12 because their temperature range was only up to 559K. We have tried

to determine the Debye-Waller factor at room temperature by measuring the relative intensities $I(hkl)/I(h_ok_ol_o)$. We did not succeed because our aluminum powder sample consisted of relatively large grains, so the orientation of crystals was not completely random, therefore the relative intensities showed significant variation from the random powder value. To determine the change of the Debye-Waller factor from room temperature, we need to know its value at room temperature. Since we could not evaluate it, we used $B_{(T=295K)} = .89$ from MacDonald [11]. We found that our results did not change significantly if we chose $B_{(T=295K)} = .90$ from Martin & O'Connor [12] or $B_{(T=295K)} = .85$ from Dingle & Medlin [10].

This work has clearly shown that the simple EDXD system at Brock University may be usefully applied to certain diffraction studies on simple crystalline materials, which have normally been done by using more sophisticated instruments.

Elyaseery [4] reported that he could not reproduce the measurements of the diffracted beam intensities at high temperature due to the inconsistency of the incident beam. We have found that our molybdenum x-ray tube produced a stable intensity radiation source. The variations in the voltage and the current of our x-ray generator was observed to be about 1KV and 1mA respectively; by making adjustments when required, these variations did not significantly effect the intensity of difffracted beam.

To make reproducible measurements of diffracted beam intensities from unpressed aluminum powder samples with grain sizes from

approximately 10μ to 40μ at room temperature, we found that it was necessary to reposition the detector scattering angle very accurately.

We were not able to obtain reproducible high temperature intensity data using unpressed samples.The unpressed sample density was 40% to 50% of that of aluminum solid. The powder was not a stable structure, so that changes in grain orientation was possible during heating/cooling and we speculated that the lack of reproducibility was caused by this.

The fluctuation of temperature readings at the beginning of our experiment was caused by bad contacts between thermocouples and the surface of the copper block.

Reproducible high temperature intensity data was obtained by using aluminum powder pressed into tablets with a density of about 80% of that of aluminum solid. Great care was also taken to maintain the thermocouples securely clamped to the tablet surface and heater assembly; this ensured sufficiently accurate and reproducible temperature measurements. To reduce effects due to any remaining changes in grain orientation in the high density tablets, the diffraction angle range accepted by the detector was increased.

Elyaseery's work [4] and our work have demonstrated that the EDXD system at Brock University is a workable system for materials with low melting point. To do measurements for materials of higher melting point or for amorphous materials at higher temperatures, it would be desirable to make some modifications:

(i) Increase the energy of the x-ray beam to 50KeV so we could

measure diffraction intensities of scattering vector **q** with high magnitude which is suitable for works on amorphous materials.

(ii) Replace the copper block heater by a stainless steel block so it could stand at higher temperature.

(iii) Replace existing heater cartridges with tungsten wires so they would not be damaged at higher temperature.

(iv) Insert thermocouples made from platinum-rhodium into the heater block for good contacts.

(v) Interfaces of the sample and the surface of the heater block could be separate by a layer of a thermal conducting compound to increase the thermal contact between them.

REFERENCES

1. Giessen, B. C. & Gordon, G. E. (1968), Science, vol. 159, 973 - 975.

2. Hoving, W., Egami, T., Vincze, I & Vander Woude, F. (1987), J. Phys, E, Scis. Instruments, vol 20, 188 - 192.

3. Egami, T. (1979), J. Appl. Phys., vol 50, 1564 - 1569.

4. Elyaseery, I. (1991),M.Sc. thesis, Brock University.

5. Killean, R. C. & Lisher, E. J.(1975), J. Phys. F: Metal Physics, vol 5, 1107 - 1112.

6. Shukla, R. C. & Hubschle, H. (1989), Solid state Communications, vol 72, 1135 - 1140.

7. Owen, E. R. & Williams, r. W. (1947), Proc. R. Soc. London, vol A188, 509 - 521.

8. Chipman, D.R.(1960), J. Appl. Phys., vol 30, 2012 - 2015.

9. Nicklow, R. W. & Young, R. A. (1966), Phys. Rev., vol 152, 591 - 598.

10. Dingle, R. E. & Medlin, E. H. (1972), Acta Cryst., vol A28, 22 - 27

11. Mac Donald, D. L. (1967), Acta Cryst., vol A23, 185 - 191.

12. Martin, C. J. & O'connor, D. A. (1978), Acta Cryst., vol A34, 500 - 505.

13. Wilson, A. J. C. (1942), Nature, vol 150, 151 - 152.

14. Killean, R. C. (1974), J. Phys. F: Metal Physics, vol 4, 1908 - 1914.

15. Kittel, C. (1976), 'Introduction to Solid state Physics', 5th edition, John Willey andd sons Ltd.

16. James, R. W. (1965), 'The Optical Principles of the Diffraction of X-ray', Bell and sons Ltd.

17. Woolfson, M. M.(1970), 'An Introduction to X-ray Crystallography', Cambridge University Press.

18. Azaroff, L. V. (1968), 'Elements of X-ray Crystallography', McGraw-Hill.

19. O'connor, D. A. & Butt, N. M. (1963), Physics Letters, vol 7, 233 - 235.

20 Albanese, G. et Al (1972), Phys. Rev. B, vol 5, 1746 - 1757.

21. Albanese, G.& Ghezzi, C. (1973) Phys. Rev B, vol 8, 1315 - 1322.

22. Willis, B. T. M (1969), Acta Cryst. , vol A25, 277 - 299.

23. Paskin, A. (1958), Acta Cryst., vol A11, 165 - 168.

24. Paskin, A. (1959), Acta Cryst.,vol A12, 290 - 294.

25. Chipman, D.R. & Paskin, A (1959), J. Appl. Phys., vol 30, 1992 - 1997.

26. Chipman, D.R. & Paskin, A (1959), J. Appl. Phys., vol 30, 1998 - 2001.

27. Touloukian, Y. C, Kirby, R. K, Taylor, R. E, Desai, P. D (1975), 'Thermal Expansion, Metallic Elements and Alloys', vol 12, of 'Thermophysical Properties of Matter',Plenum Press.